Journal of Cleaner Production 372 (2022) 133752

Contents lists available at ScienceDirect

Journal of Cleaner Production

journal homepage: www.elsevier.com/locate/jclepro

Design and sustainability analyses of road base layers stabilized with traditional and nontraditional additives

Diego Maria Barbieri [a,*], Baowen Lou [a,b], Robert Jason Dyke [c], Xueting Wang [b], Hao Chen [a], Benan Shu [d], Uneb Gazder [e], Suksun Horpibulsuk [f,g], Jeb S. Tingle [h], Inge Hoff [a]

[a] Norwegian University of Science and Technology, Department of Civil and Environmental Engineering, Høgskoleringen 7A, Trondheim, 7491, Trøndelag, Norway
[b] Chang'an University, School of Materials Science and Technology, Nan Er Huan Road (Mid-section), Xi'an, 710064, Shaanxi, China
[c] Oslo Metropolitan University, Department of Civil Engineering and Energy Technology, Pilestredet 35, Oslo 0166 Norway
[d] Foshan Transportation Science and Technology Co. Ltd, Kuiqi Second Road 18, Foshan, 528000, Guangdong, China
[e] University of Bahrain, Department of Civil Engineering, Isa Town, 32038, Bahrain
[f] Suranaree University of Technology, School of Civil Engineering, 111 University Avenue, Muang District, 30000, Nakhon Ratchasima, Thailand
[g] The Royal Society of Thailand, Academy of Science, Sanam Suea Pa, Dusit, 10300, Bangkok, Thailand
[h] U.S. Army Engineer Research and Development Center, Geotechnical and Structures Laboratory, 3909 Halls Ferry Road, Vicksburg, 39180, Mississippi, United States

ARTICLE INFO

Handling Editor: Zhen Leng

Keywords:
Road stabilization
Pavement geotechnics
Freeze-thaw cycles
Thickness reduction
Carbon dioxide emission
Construction cost

ABSTRACT

Base course is an important structural layer of a road pavement which plays a vital role in transferring and distributing the traffic loadings to the subgrade. The base usually comprises unbound materials, which can be stabilized to enhance the mechanical properties when necessary. This study evaluates all the various types of stabilization products suitable for a coarse-graded base, which can be grouped as traditional solutions (cement and bitumen) and nontraditional solutions (brine salt, clay, organic non-petroleum, organic petroleum and synthetic polymer). The research presented here addresses four major objectives. First, the effect of the stabilizers is evaluated via cyclic triaxial tests both before and after the exposure of the samples to ten freeze-thaw cycles. Second, the potential to reduce the thickness of a base course is evaluated for each stabilizer according to the Norwegian pavement design code. Third, the study appraises the associated reductions in carbon dioxide emissions during the operations for road construction in Norway and, finally, the related economic costs are derived. The freeze-thaw actions exert almost no effect on the samples stabilized with cement, bitumen, organic petroleum and synthetic polymer. These stabilizers seem to display an aging effect, which is responsible for the improvement of the mechanical properties over time. The required thickness of a stabilized base layer is at least halved compared to a traditional unbound course and this remarkably lowers the carbon footprint of the construction operations. The application of most of the stabilizers is cost-effective, whereas their market price and the transport distance of aggregates are two crucial factors for the determination of their economic competitiveness.

1. Introduction

1.1. Background

The structure of a road pavement comprises several courses designed to transfer the trafficking loads to the natural subgrade at the bottom. Typically, the upper courses (i.e., surface and binder layers) are bound using bitumen or cement, while the other courses (i.e., base, subbase and frost protection layers) are generally solely comprised of unbound aggregates, namely Unbound Granular Materials (UGMs) (Huang, 2004; Mallick and El-Korchi, 2013; Thom, 2014). Moreover, an UGM course can be directly employed as a top layer when the Annual Average Daily Traffic (AADT) is sufficiently low, generally smaller than 1000 vehicles/day (Aursand and Horvli, 2009; Douglas, 2016; Silyanov et al., 2020), for so-called Low-Volume Roads (LVRs). The estimated length of the world road network is reported to be 22 million km and

* Corresponding author.
E-mail addresses: diegomb271@gmail.com (D.M. Barbieri), loubaowen@chd.edu.cn, loubaowen@chd.edu.cn (B. Lou), dykej.robert@gmail.com (R.J. Dyke), wxting@chd.edu.cn (X. Wang), hao.chen@ntnu.no (H. Chen), shuba@whut.edu.cn (B. Shu), ugazder@uob.edu.bh (U. Gazder), suksun@g.sut.ac.th (S. Horpibulsuk), jeb.s.tingle@usace.army.mil (J.S. Tingle), inge.hoff@ntnu.no (I. Hoff).

https://doi.org/10.1016/j.jclepro.2022.133752
Received 15 June 2022; Received in revised form 3 August 2022; Accepted 19 August 2022
Available online 26 August 2022

approximately 14 million km can be classified as LVRs (Meijer et al., 2018; Silyanov and Sodikov, 2017). Considering the extent of the LVR network as well as the global need for efficient and resilient pavement infrastructure, it is straightforward to understand the importance of properly designing, constructing and maintaining unbound layers of road pavements (Barbieri et al., 2017).

Due to continual increases in traffic loads and changes in environmental conditions, innovative technologies are sought to improve the mechanical properties of unbound course materials to provide enduring solutions (Arulrajah et al., 2013; Gomes Correia et al., 2016; Horpibulsuk et al., 2012). In-situ stabilization has long been used as a cost-effective technology to improve the mechanical response of UGMs by means of cold recycling/mixing process (Latifi et al., 2018). Numerous stabilizers are available on the global market (Jones, 2017) and they can be divided into traditional solutions (such as cement and bitumen) and nontraditional solutions (brine salt, clay, organic non-petroleum, organic petroleum, synthetic polymer and concentrated liquid) (Tingle et al., 2007).

1.2. Current research status

While a myriad of geomaterial stabilization technologies has been characterized with results available in many publications and reports, currently there is a surprising paucity of research efforts *simultaneously* comparing the performance of different traditional and nontraditional stabilizers *in a single study* under the same test conditions. As reviewed in a previous study by the authors (Barbieri et al., 2022b), the few available works in this regard have characterized the various degrees of stabilization in the laboratory, mostly using Unconfined Compression Strength (UCS) and California Bearing Ratio (CBR) tests (Blanck et al., 2014; Bushman et al., 2005; Santoni et al., 2002; Tingle and Santoni, 2003), or in the field, with structural assessments using deflectometers (Barbieri et al., 2021b; Beaulieu et al., 2014; Li et al., 2019).

Possible degradations in the mechanical behavior due to water exposure as well as freezing and thawing are particularly significant in cold regions. Such actions can largely impair the performance of roads and eventually cause major distresses if proper countermeasures are not taken (Dawson, 2008; Simonsen et al., 2002; Simonsen and Isacsson, 1999). As reported in Table 1, the experimental investigations *simultaneously* comparing *in a single study* the performance of geomaterials treated with traditional and nontraditional stabilizers after the exposure to Freeze-Thaw (FT) cycles are remarkably scarce.

Another important aspect to address when applying road stabilizers is the evaluation of the associated environmental impact and economic cost. From a Life Cycle Analysis (LCA) perspective, the life of a road infrastructure can be broken down in four stages: production, construction, use and end-of-life (CEN, 2022, 2019a). The production stage is composed by material manufacturing and material supply phases, while the construction stage comprises transport and installation phases. Focusing on these two stages, Table 2 reports the experimental investigations *simultaneously* comparing *in a single study* the carbon dioxide emissions and/or the economic costs of geomaterials for road pavements stabilized with traditional and nontraditional technologies. There is a considerable paucity of existing works delving on these matters.

While some guidelines for selection and application of stabilizers have been developed (Barnes et al., 2014; Kestler, 2009; Lunsford and Mahoney, 2001; White and Vennapusa, 2013), there is a lack of standardized procedures for the thorough assessment of nontraditional technologies. Thus, the absence of widely accepted standards for stabilized materials limits their routine inclusion in national pavement design guidelines. As a result, pavement engineers are often (with good reason) reluctant to employ innovative products in real operations.

As reported in Tables 1 and 2, this research systematically compares the stabilization potential of traditional and nontraditional technologies that can improve the mechanical properties of coarse-graded unbound materials. Lime and concentrated liquid products (high-acidity and low-

Table 1
Overview of the experimental investigations *simultaneously* comparing *in a single study* the mechanical performance of geomaterials stabilized with traditional and nontraditional technologies after freeze-thaw cycles.

	MATERIAL		INVESTIGATED STABILIZERS								PERFORMED EXPERIMENTAL TESTS					
			TRADITIONAL		NONTRADITIONAL						LABORATORY			FIELD		
			CEMENT	BITUMEN[a]	LIME[b]	BRINE SALT	CLAY[a]	ORGANIC NON-PETROLEUM	ORGANIC PETROLEUM	SYNTHETIC POLYMER	CONCENTRATED LIQUID[b]	UNCONFINED COMPRESSION TEST	CBR TEST	TRIAXIAL TEST	FALLING WEIGHT DEFLECTOMETER	DYNAMIC CONE PENETROMETER
(Pierre et al., 2008)	sandy gravel		X			X				X		✓	✓	✓		
(Li et al., 2017)	silty clay		X		X	X	X								✓	✓
(Li et al., 2021)	silt				X	X		X				✓				
this study	sandy gravel		X	X		X	X	X	X	X				✓		

[a] Mostly effective for coarse-graded material.
[b] Mostly effective for fine-graded material.

acidity emulsions) are not considered in this study since they are reported to be more appropriate for stabilizing fine-graded geomaterials (Jones, 2017; Tingle et al., 2007). Finally, the cement considered in this study is Ordinary Portland Cement (OPC). In this regard, it is important to highlight that geopolymers, also referred to as alkali-activated materials, represent new alternative cementitious resources which are likely to gradually replace OPC (Amran et al., 2020; Mohajerani et al., 2019; Xiao et al., 2020a, 2021, 2022). Few recent studies have shed light on the beneficial environmental and mechanical effects when employing geopolymers to stabilize road bases (Poltue et al., 2020; Xiao et al., 2020b; Zhang et al., 2021).

1.3. Novelty and structure of the study

This research pivots on the main concerns regarding the application of traditional and nontraditional stabilizers for road construction aggregates: improved mechanical properties, resistance to external actions as well as sustainable and economically competitive construction operations (Balaguera et al., 2018; Blanck et al., 2016; Celauro et al., 2015; Praticò et al., 2011). Eventually, this work aims to develop a deeper confidence towards the use of nontraditional products among road agencies, professionals and stakeholders to provide longer design life for pavements as well as reduce associated costs and carbon emissions. The conceptual diagram of the investigation is depicted in Fig. 1.

The mechanical responses of stabilized aggregate specimens are assessed via Repeated Load Triaxial Tests (RLTTs) in terms of elastic stiffness and resistance to permanent deformation (CEN, 2004). Furthermore, to attain a more comprehensive understanding of the stabilization durability, the RLTTs are performed both before and after the exposure of the samples to 10 FT cycles. Differently from other most common and rapid experimental procedures like UCS and CBR tests (Araya et al., 2010), RLTT is non-destructive and the obtained results can be directly implemented into a mechanistic-empirical road design (Alnedawi et al., 2022; Chowdhury and Kassem, 2022; Ghadimi and Nikraz, 2017; Titi and Matar, 2018). As reported in Table 1, only one previous study has employed RLTT to compare the effects of traditional and nontraditional soil stabilizers in connection with FT cycles (Pierre et al., 2008). Nevertheless, in that research the performed RLTT procedure was simplified and only few stabilizers were investigated in comparison to the present investigation.

Conservatively considering the RLTT results of stabilized specimens demonstrating good resistance against FT actions, this research evaluates the possibility of reducing the thickness of a stabilized base layer when compared with a traditional UGM base layer according to the Norwegian pavement design code "N200" (NPRA, 2018, 2014). A reduction in the base layer thickness limits carbon footprints and lowers economic costs associated with road construction. The decrease in carbon dioxide emissions and associated costs are appraised using "HERMES CO_2" spreadsheet tool (Barbieri et al., 2021c). As documented in Table 2, this research contributes to fill the very remarkable gap related to the assessment of carbon footprints generated during road construction with traditional and nontraditional stabilizers. As for the appraisal of associated economic costs, two previous studies reported extremely concise information in this regard (Li et al., 2019; Uys et al., 2011). Differently, this work extensively analyses and discusses the economic aspects employing "HERMES CO_2" spreadsheet tool. Furthermore, this research considers the variability in the transport distance to move the aggregates from the resource site to the construction site.

2. Materials

The gradation of the coarse-grained samples tested in this study is reported in Table 3, which indicates the sizes between 0 mm and 30 mm as commonly adopted for base layers in flexible pavements (NPRA, 2018, 2014). The used UGM has good mechanical properties (Los-Angeles LA = 18.2, micro-Deval MDE = 14.2) (CEN, 2011, 2010) with very high resistance to freezing cycles (category F1) (CEN, 2019b, 2007). The tested UGM was collected from a quarry located in Trøndelag region. The aggregates, mainly comprising fine-grained gabbro/metagabbro, are widely employed for road construction purposes in central Norway and Sweden thanks to their abundant availability (Grenne et al., 1980; Petkovic et al., 2004).

The technologies reported to be effective in stabilizing coarse-graded aggregates were selected for this research (Jones, 2017), they include traditional (cement, bitumen) and nontraditional (brine salt, clay, organic non-petroleum, organic petroleum, synthetic polymer) stabilizers. The water content and cost of each of these technologies are listed in Table 4. A detailed description of the tested material as well as the physical and chemical properties of the stabilizers can be found elsewhere (Barbieri et al., 2022a, 2022b; Tingle et al., 2007). Furthermore, the products included in this study are associated with a degree of toxicity ranging from none to moderate (Kunz et al., 2021). Having tested the mechanical response of only one geological type of construction aggregates represents a minor limitation of this study. For coarse-graded geomaterials, the stabilization process mainly occurs thanks to the physical cementation hinging upon the rock particles size. Differently, chemical effects are predominant when stabilizing fine-graded geomaterials (e.g., silt, clay) and in this case it would be advisable to compare the mechanical responses associated with different geologies (Tingle et al., 2007).

3. Experimental Methodology

3.1. Repeated load triaxial test

The RLTT is a laboratory investigation method that enables a thorough assessment of the mechanical properties of bound and unbound aggregates by characterizing the elastic and plastic responses for a wide variety of stress state (Lekarp et al., 2000a, 2000b).

3.1.1. Specimen preparation and testing

Two replicate specimens (sample 1 and sample 2) were tested for each of the fourteen unique stabilizers. To assess a possible variation in the mechanical response due to freezing-thawing actions, the same RLTT samples were tested both before and after the exposure to FT cycles. In addition, two replicates of unstabilized UGM specimens were also tested to provide a baseline. Table 5 details the application rate in terms of dry mass of each stabilizer. Whenever possible, the same percentage was adopted to enable an "apple-to-apple" comparison. In fact, it can be noted that the most used content was 1.2%, while cement and bitumen were applied at higher rates, 4% and 3% respectively, as generally undertaken in real construction projects (Myre, 2000; Plati, 2019; Tan et al., 2020). Anyway, it is important to stress that the stabilizer content was not optimized for performance or cost but selected after some trial-and-error procedures to achieve entire coating of the particles surface. When it came to brine salt SAL-B, a quantity of 0.2% was mixed with cement CEM. Except for the aggregates stabilized by means of bitumen BIT, cement CEM, minerals mixture salt SAL-B and polyurethane POL, the initial amount of water contained in the RLTT samples was $w = 5\%$, which corresponded to the Optimum Moisture Content (OMC) (CEN, 2003). Referring to bentonite BEN, an amount of 0.4% by mass was employed to obtain a workable slurry when blended with $w = 5\%$. As reported in Table 5, the quantity of water already contained in the concentrated form of every stabilizer was taken into consideration when creating specimens at OMC. The additives were carefully blended with water using a high-shear mixer.

The main steps of the procedure undertaken to create RLTT samples are illustrated in Fig. 2. The quantity of aggregates forming each specimen was approximately 12 kg and it was equally split in five batches stored in as many plastic bags. In order to create a uniform RLTT sample, the grading curve of the material in every batch was the same. Each additive was mixed with the rock aggregates at room temperature

Table 2
Overview of the experimental investigations *simultaneously* comparing *in a single study* the carbon dioxide emissions and/or the economic costs of geomaterials for road pavements stabilized with traditional and nontraditional technologies.

	MATERIAL	INVESTIGATED STABILIZERS						
		TRADITIONAL			NONTRADITIONAL			
		CEMENT	BITUMEN[a]	LIME[b]	BRINE SALT	CLAY[a]	ORGANIC NON-PETROLEUM	ORGANIC PETROLEUM
(Uys et al., 2011)	silty clay	X	X				X	
(Zhang et al., 2017)	silt			X			X	
(Khoeini et al., 2019)	sandy gravel		X					
(Li et al., 2019)	silty sand	X		X	X	X		
this study	sandy gravel	X	X		X	X	X	X

[a] Mostly effective for coarse-graded material.
[b] Mostly effective for fine-graded material.

according to the percentage specified in Table 5 and the plastic bags were carefully shaken manually. The only exception was represented by the aggregates treated with bitumen; in this case, both the aggregates and the binder were preheated at 155 °C and the blending was performed by a hot rotating mixer. The five batches used to create a single specimen were compacted inside a steel mold employing a Milwaukee 2″ SDS Max rotary hammer and the average bulk density was 2.4 t/m^3 (CEN, 2003). A dedicated tool was employed to eject the sample and one latex membrane was applied at this stage. Finally, the specimens were cured in temperature-controlled cabinets as documented in Table 5 to let the water evaporate and let each additive attach properly to the aggregates. To facilitate such drying process, the latex membrane was carefully rolled manually at regular time intervals either upwards or downwards to increase the amount of the specimen surface exposed to air. Further detailed numerical and visual information regarding the specimen preparation, i.e., material quantities, compaction rate as well as used tools and molds, is available elsewhere (Barbieri et al., 2021a, 2022a, 2022b).

To assess the effectiveness of each stabilizer when exposed to possible detrimental environmental conditions such as freezing, the treated samples were tested dried both before and after the exposure to 10 FT cycles. In light of the non-destructive nature of RLTT and the relatively low associated stress levels (Arulrajah et al., 2020; Gidel et al., 2001; Han et al., 2019; Islam et al., 2020), the same specimens were tested to compare the mechanical behavior before and after the freezing-thawing actions. The chosen amount of FT cycles is consistent with previous studies (Bassani and Tefa, 2018; Domitrović et al., 2019; Ghorbani et al., 2020) and sufficient to characterize the response to freeze-thaw durability, which usually levels off after a few repetitions (Akbas et al., 2021; Qu et al., 2019; Rosa et al., 2017; Tian et al., 2019). Water capillary rise was not likely to occur due to the coarse-graded nature of the specimens (Dawson, 2008). The following conditioning procedures were performed at ordinary atmospheric pressure for each FT cycle, as depicted in Fig. 3: submersion in water (23 °C, 5 min), retrieval of the sample and release of water excess (23 °C, 5 min), unsaturated freezing (−15 °C, 24 h) and following water thawing (23 °C, 24 h). The submersion of the specimen was the only step when the sample had access to water, which could circulate in the accessible pores through the rooms present at the extreme ends. These ends were also used to insert thermocouples during the freezing stage after 8 h and 24 h to ascertain that the temperature inside the sample was −15 °C. Handling disturbances were limited by the fastener system and the very careful execution of such laboratory operations. The duration of the immersion in water was only 5 min considering the coarse-graded nature of the aggregates; however, future research can also consider longer time. The time span between the first (Barbieri et al., 2022a, 2022b) and the second rounds of testing, namely before and after FT cycles, was 6 months. FT cycles were performed during the fifth month and the samples were then dried in a ventilated cabinet for seven days before the final testing. It is important to stress that, due to the possible aging of the stabilized specimens that may have naturally occurred during the six-month temporal span, the final RLTT results may also include any natural variations in the mechanical responses independent from freezing-thawing actions.

A Multi-Stage Low Stress Level (MS LSL) loading procedure was applied to perform RLTT (CEN, 2004; Gidel et al., 2001). MS LSL specifies a series of five loading sequences based on combinations of the static triaxial or confining stress σ_3, exerted with pressurized water, and a dynamic deviator or vertical stress σ_d, exerted with a hydraulic piston. Each load test sequence includes six load steps and each load step consists of 60 000 load pulses applied at a rate of 10 Hz. Linear Variable Differential Transducers (LVDTs) were used to measure the axial deformations of the specimens and the LVTDs were regularly calibrated after every test using a Mitutoyo calibration gauge.

The time required to prepare each sample and perform its corresponding RLTT was approximately 11 h; the testing device was always under human supervision to adjust the levels of confining stress σ_3. It is important to stress that it would have been preferable to increase the number of replicate tests from two to three or even more to obtain more experimental data. However, due to the laborious nature of the testing as well as time and cost limitations inside the frame of the project, the number of replicate specimens for the RLTT was limited to two. It was preferred to cover a wider array of stabilizers instead of focusing on few ones with more samples. More detailed information regarding the employed equipment, measuring instrumentation and data attainment can be found elsewhere (Barbieri et al., 2021a). The RLTT device setup is depicted in Fig. 4. Every step related to the creation, testing and handling of RLTT specimens illustrated in this subsection was scrupulously performed by the same experienced researcher to avoid the occurrence of random errors.

3.1.2. Results interpretation

MS LSL cyclic triaxial tests provide data to assess the elastic stiffness and permanent deformation of the specimens. The elastic stiffness, also known in road engineering as resilient modulus M_R, is defined as follows for a given constant σ_3

$$M_R = \frac{\Delta\sigma_{d,\,dyn}}{\varepsilon_{el,a}} \tag{1}$$

where the numerator and the denominator refer to dynamic deviator stress $\sigma_{d,dyn}$ and the elastic axial strain, respectively. The experimental data were analyzed using the Hicks & Monismith model (Chowdhury, 2021; Hicks and Monismith, 1971; Lekarp et al., 2000a) considering a reference pressure $\sigma_a = 100$ kPa

INVESTIGATED STABILIZERS		CO_2 EMISSIONS				ECONOMIC COSTS			
NONTRADITIONAL		PRODUC. STAGE		CONSTR. STAGE		PRODUC. STAGE		CONSTR. STAGE	
SYNTHETIC POLYMER	CONCENTRATED LIQUID[b]	MATERIAL MANUFACTURING	MATERIAL SUPPLY	TRANSPORT	INSTALLATION	MATERIAL MANUFACTURING	MATERIAL SUPPLY	TRANSPORT	INSTALLATION
X	X						✓	✓	✓
							✓		
X							✓		
							✓	✓	✓
X				✓	✓		✓	✓	✓

$$M_R = k_1 \sigma_a \left(\frac{\theta}{\sigma_a}\right)^{k_2} \tag{2}$$

where θ is the sum of the principal stresses σ_1, σ_2, σ_3 ($\sigma_2 = \sigma_3$) and the constants k_1, k_2 are regression coefficients. Although the Hicks & Monismith formulation was conceived almost fifty years ago, this model is largely employed in the research community as it efficiently describes the trend of experimental data in a two-dimensional plane. Furthermore, the Hicks & Monismith model is needed to perform the calculations indicated by the pavement design code "N200" as reported in section 3.2.

For the interpretation of the plastic axial deformations developed during RLTT, the Hyde model takes into consideration the deviator stress σ_d and the triaxial confining stress σ_3 as follows (Hyde, 1974)

$$\varepsilon_{pl,a} = a_{HY} \frac{\sigma_d}{\sigma_3} \tag{3}$$

where a_{HY} is the regression coefficient. Alternatively, the deformation response can be assessed referring to the shakedown theory (Alnedawi et al., 2019; Tao et al., 2010; Werkmeister et al., 2005) in the form of Coulomb formulation (Cerni et al., 2012; Hoff et al., 2003). Every RLTT loading step is classified according to three possible ranges, which are defined by calculating the plastic strain rate $\dot{\varepsilon}_{pl}$ for the last 5 000 to 10

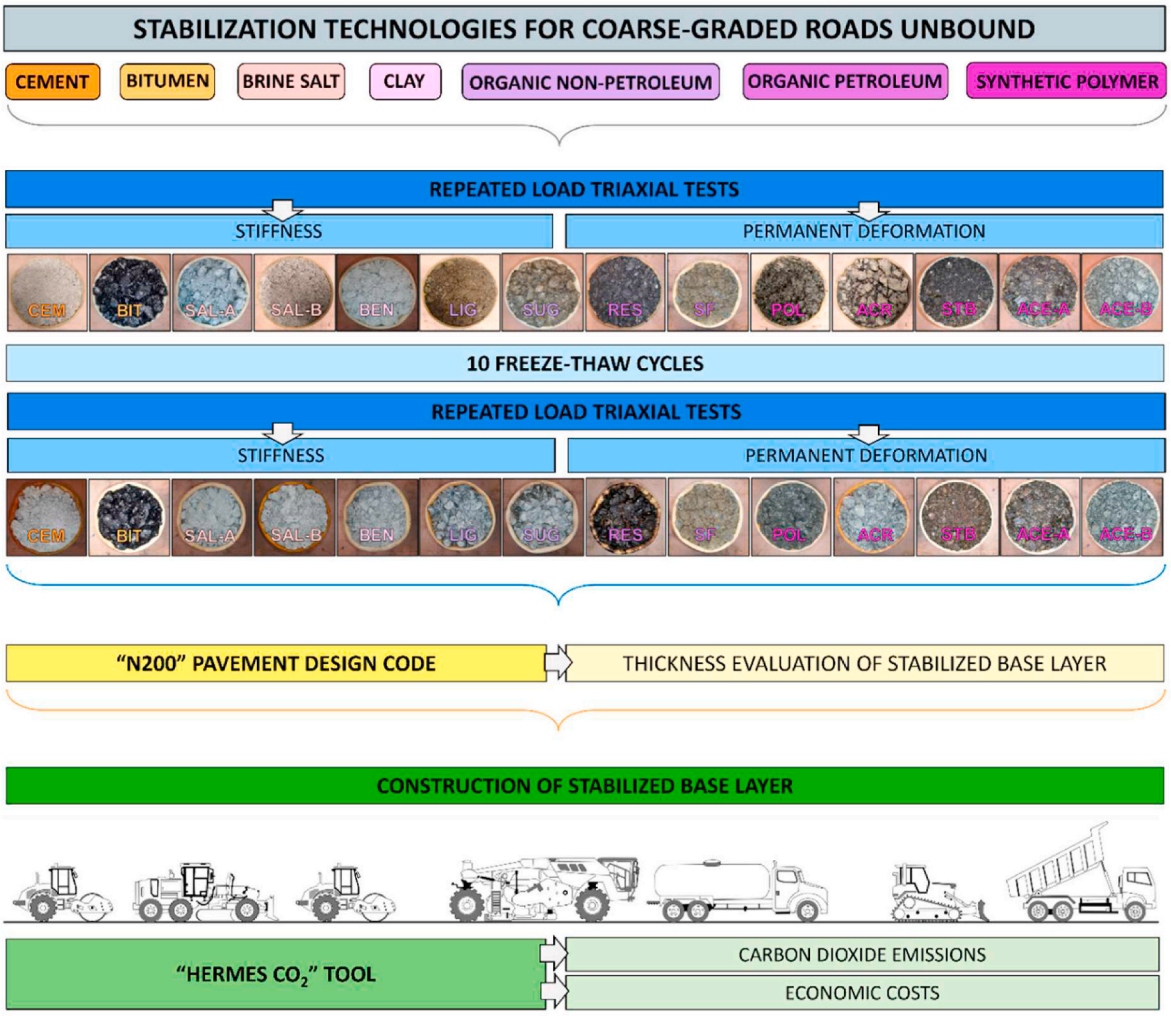

Fig. 1. Flowchart of the study.

000 cycles: range A or plastic shakedown ($\dot{\varepsilon}_{pl} < 2.5 \cdot 10^{-8}$), range B or plastic creep ($2.5 \cdot 10^{-8} < \dot{\varepsilon}_{pl} < 1.0 \cdot 10^{-7}$) and range C or incremental collapse ($\dot{\varepsilon}_{pl} > 1.0 \cdot 10^{-7}$). On the one hand, range A is associated with a plastic response for a finite amount of load cycles after which the deformation is purely elastic. On the other hand, range C indicates increasing plastic deformations resulting from additional load applications. Range B is related to an intermediate behavior characterized by stable and relatively small accumulation of plastic strain.

3.2. Design of stabilized road base layers

The study considers the construction of unstabilized and stabilized base layers for a road pavement in Norway. The pavement design code "N200" utilizes a mechanistic-empirical approach to design flexible road layers using load distribution coefficients to be selected based on several parameters. The code is issued by the Norwegian Public Roads Administration (NPRA) and is valid in both Norway and Iceland. The required inputs consist mainly of the design traffic volume and properties of the anticipated construction materials (NPRA, 2018, 2014). The design process is typically comprised of the steps illustrated in Fig. 5.

The design procedure of code "N200" takes into consideration the sum of equivalent 10-ton axles N, which is defined as

$$N = 365 \cdot C \cdot E \cdot AADT_H \cdot f \cdot \frac{(1 + 0.01 \cdot r)^n - 1}{0.01 \cdot r} \quad (4)$$

with C as the average number of axles per heavy vehicle (generally $C = 2.4$), E as an average equivalent factor for the axles of heavy vehicles (generally $E = 0.427$), $AADT_H$ the daily average number of heavy vehicles, r the yearly traffic increment, n the road lifespan and f the lane distribution factor. The traffic group is defined based on the value of the sum of equivalent 10-ton axles N as detailed in Table 6.

The thickness of the wearing course plus the binder course is defined based on the AADT during the first year: 3.0 cm + 3.0 cm for AADT <1 000, 3.5 cm + 3.0 cm for 1000 < AADT <3 000, 4.0 cm + 3.0 cm for 3000 < AADT <5000 and 4.0 cm + 4.0 cm for 5000 < AADT. Different types of construction materials can be used in the base layer depending upon the traffic volume. This study considers traffic group A, where the crushed rock aggregates ("*knust berg*" in Norwegian) are used and the thickness is 20 cm. Each layer within the pavement structure is given a "load distribution coefficient" ("*lastfordelingskoeffisient*" in Norwegian) a. For the materials selected in this study, a is equal to 3 and 1.35 for the top layers (wearing course, binder course) and for the base layer, respectively. Finally, the "base layer index" ("*bærelagindeks*" in Norwegian) BI of these three layers is estimated as

$$BI = \sum_{i=1}^{N} t_i \cdot a_i \quad (5)$$

where i refers to the generic i-th layer, t is the layer thickness in cm and a is the load distribution coefficient. The base layer index BI must be larger than a minimum threshold BI_{min} defined by the code, which is equal to 39 for the scenario described in this study.

The load distribution coefficients a are specified for several different types of road construction materials, but there are no values provided for stabilized aggregates. In this regard, the code "N200" allows for the estimation of a unique a parameter by means of RLTTs according to the following formula deriving from the bending theory for elastic plates (Das, 2014; Huang, 2004)

Table 3
Gradation curve of UGM used for creating RLTT samples, adapted from (Barbieri et al., 2022a, 2022b).

Sieve (mm)	0.063	0.25	2	16	22.4	31.5	45
Passing (%)	4	6	16	40	65	95	100

Table 4
Denomination, contained water and price estimates of the investigated stabilizers, adapted from (Barbieri et al., 2022a, 2022b).

Category	Type	Code	w content (%)	Price (EUR/kg)
CEMENT	cement C20	CEM	0	0.3
BITUMEN	bitumen 70/100	BIT	0	0.5
BRINE SALT	calcium chloride	SAL-A	23	0.3
	minerals mixture[a]	SAL-B[a]	7	11.0
CLAY	bentonite	BEN	0	1.2
ORGANIC NON-PETROLEUM	lignosulfonate	LIG	50	0.2
	reduced sugar	SUG	52	1.4
ORGANIC PETROLEUM	petroleum resin	RES	20	1.5
	synthetic fluid	SF	0	3.3
SYNTHETIC POLYMER	polyurethane	POL	0	4.0
	acrylate[b]	ACR[b]	48	0.6
	styrene butadiene	STB	40	3.9
	acetate type A	ACE-A	51	3.6
	acetate type B	ACE-B	44	3.7

[a] Used in addition to CEM.
[b] Bicomponent technology.

$$a = 0.17 \sqrt[3]{E_{200}} \quad (6)$$

where E_{200} is the value of the resilient modulus expressed in kPa for a bulk stress θ equal to 200 kPa assessed using the Hicks & Monismith model. The coefficient a should be rounded to the nearest 0.05 and must not lie 0.75 above the standard value a_{UGM} for the corresponding unstabilized material UGM. Considering that the design code defines a_{UGM} equal to 1.35, the maximum acceptable value of a for stabilized aggregates is 2.10.

Finally, the design approach illustrated in this section derives from the "Guide for Design of Pavement Structures" issued by the American Association of State Highway and Transportation Officials (AASHTO, 1993). In this code, each road course is associated with a layer coefficient a, which, together with its layer thickness D, contributes to define the pavement structural number SN. In a similar manner to Equation (6), the AASHTO pavement design procedure also allows for the determination of layer coefficients based on RLTT results analyzed with Hicks & Monismith model (AASHTO, 1986). Nevertheless, the "Guide for Design of Pavement Structures" does not specify which value of bulk stress θ should be considered for the assessment of resilient modulus E, whereas the code "N200" clearly sets this evaluation for $\theta = 200$ kPa. Therefore, the results of this research can be extended to any study which applies AASHTO procedure by means of the layer coefficients.

3.3. Assessment of carbon dioxide emissions and construction costs

The assessment of carbon dioxide emissions CDE and economic costs related to the construction operations of unstabilized and stabilized base layers is performed by employing the "HERMES CO_2" spreadsheet (Barbieri et al., 2021c). This tool evaluates the carbon footprints generated during a road lifespan as also documented by other studies (Pranav et al., 2022; Prasara-A and Bridhikitti, 2022). In this research, the focus is on the construction of a flexible pavement base layer and consequently only the "BASE" worksheet of the "HERMES CO_2" spreadsheet is used. Therefore, as a limitation of this study, it is reiterated that the carbon dioxide emissions are *only* calculated for the operations necessary to build the road, but not for the processes related to material procurement (e.g., production of each stabilizer).

A typical construction train for building a Norwegian road with a stabilized base course is depicted in Fig. 6 (Douglas, 2016; NPRA, 2018, 2014). Dump trucks transport the aggregates from the source and dozers

Table 5
Application rate of the stabilizers, initial water content at RLTT specimen creation, curing time and curing temperature, adapted from (Barbieri et al., 2022a, 2022b).

		CEM	BIT	SAL-A	SAL-B[a]	BEN	LIG	SUG	RES	SF	POL	ACR	STB	ACE-A	ACE-B
Application rate (%, mass)		4.0	3.0	1.2	0.2	0.4	1.2	1.2	1.2	1.5	4.5	1.2	1.2	1.2	1.2
Initial water (%, mass)		2.4	0.0	5.0	2.4	5.0	5.0	5.0	5.0	5.0	0.0	5.0	5.0	5.0	5.0
Curing	**Time (day)**	28	2	7 + 1	28	7 + 1	7 + 1	7 + 1	7 + 1	30	2	7 + 1	7 + 1	7 + 1	7 + 1
	Temperature (°C)	22	22	55 + 22	22	55 + 22	55 + 22	55 + 22	55 + 22	22	22	55 + 22	55 + 22	55 + 22	55 + 22

[a] *Used in addition to CEM.*

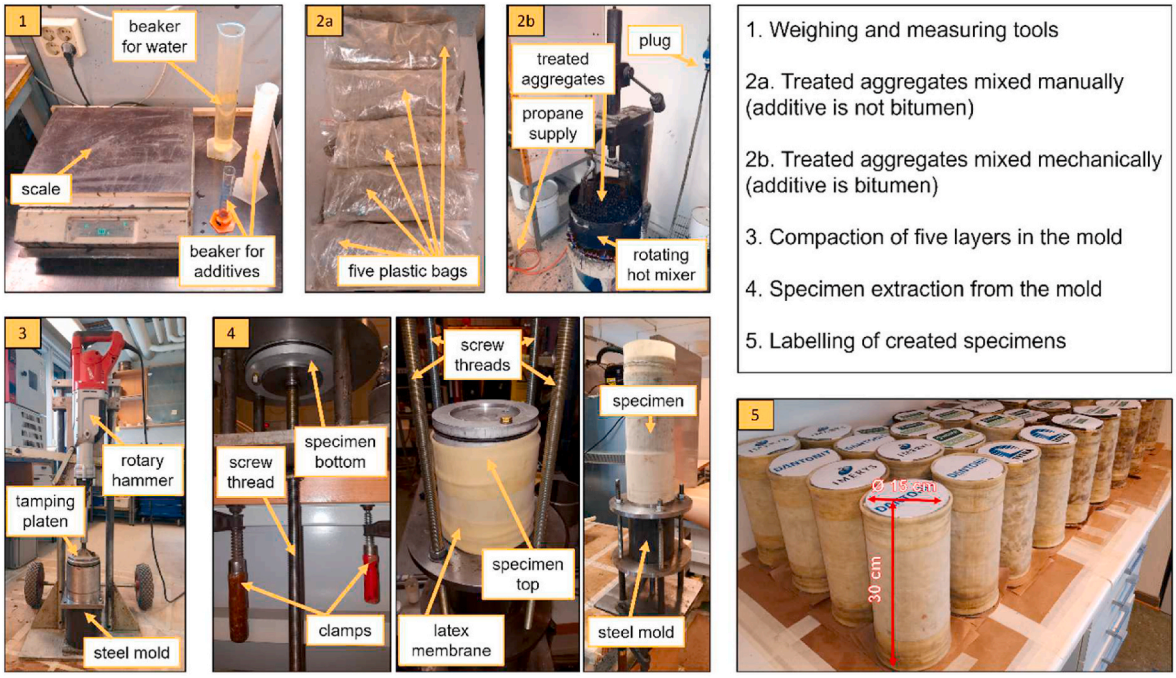

Fig. 2. Main steps to create RLTT samples.

spread them on the subbase or subgrade layer. A spreader truck feeds the reclaimer/stabilizer mixer with the designed amount of stabilizer and water. A breakdown roller follows to provide initial compaction of the stabilized layer. Then, a motor grader is used to fine-grade the surface and establish longitudinal and transverse grades. Finally, a second roller provides final compaction of the stabilized surface and achieve target density. Anyway, as the "HERMES CO_2" tool can be freely edited, different quantity and/or types of earthwork machines can be specified by the user.

The *CDE* generated by the earthwork machines can be expressed as (Heidari and Marr, 2015; Muresan et al., 2015; Trani et al., 2016)

$$CDE\left(\frac{kg}{m^3}\right) = FC\left(\frac{l}{m^3}\right)\cdot EF_{dsl} \tag{7}$$

with *FC* the fuel consumed and EF_{dsl} the emission factor for diesel (2.60 kg of CO_2 per liter). *FC* can be assessed as

$$FC\left(\frac{l}{m^3}\right) = P(kW)\cdot SC\left(\frac{kg}{kWh}\right)\cdot LF\cdot\frac{1}{\rho_f\left(\frac{kg}{l}\right)}\cdot Pr\left(\frac{h}{m^3}\right) \tag{8}$$

with *P* the power, *SC* the engine specific consumption, *LF* the load factor, ρ_f the density of the fuel (0.85 kg/l) and *Pr* the productivity. *LF* is a function of soil density and slope as well as the working duration of the

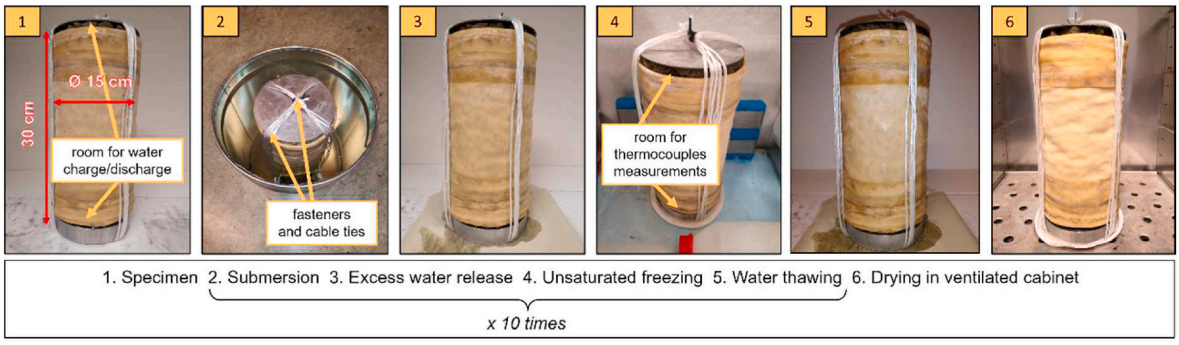

Fig. 3. Main steps to undertake FT cycles.

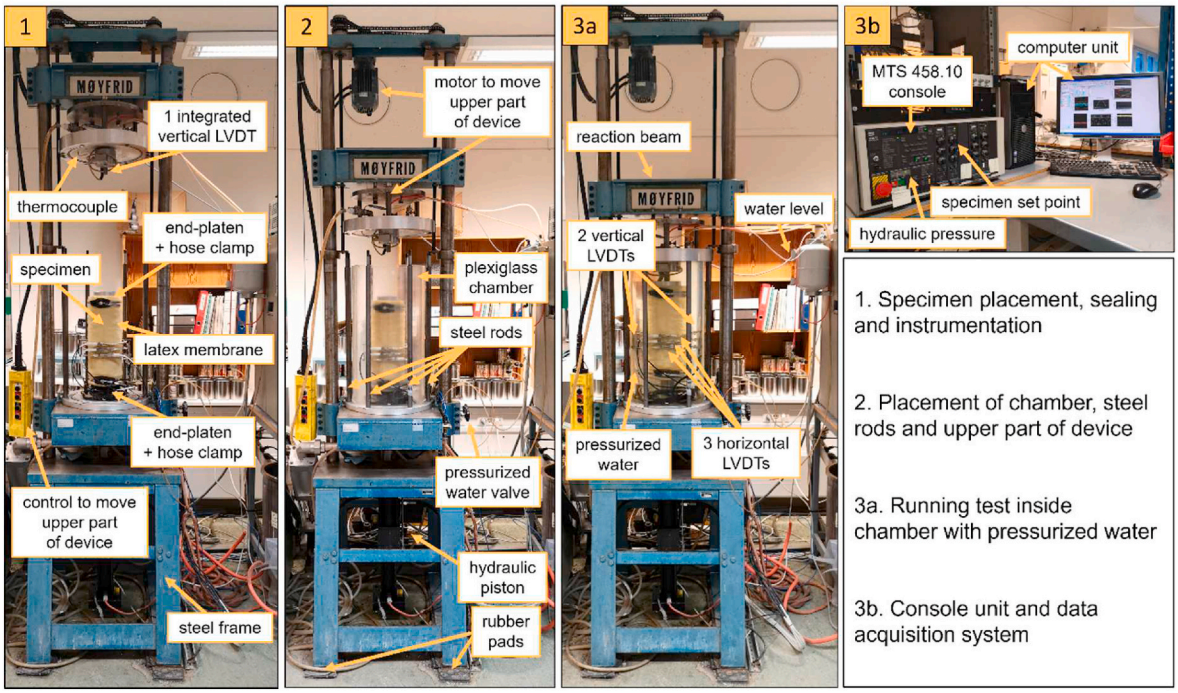

Fig. 4. Triaxial testing setup.

machine (Frey et al., 2010). When it comes to trucks, the emission factor FC_{tr} can be calculated as

$$FC_{tr}\left(\frac{l}{m^3}\right)=\frac{K\cdot R(km)\cdot Ic\left(\frac{l}{km}\right)}{C(m^3)} \quad (9)$$

with K as a coefficient related to a fully loaded truck ($K = 1.7$), R as the average distance travelled, Ic as a fuel consumption index and C the vehicle capacity.

Since the "HERMES CO_2" software can be customized by users, the worksheet "BASE" has been properly edited to include the operational costs of the earthmoving machines. These prices have been obtained by consulting with the largest Norwegian companies providing rental equipment including operators (CRAMO, 2022; PON-CAT, 2022; RAM-IRENT, 2022; Utleiesenteret, 2022). Table 7 details the main features of the chosen representative equipment set (Caterpillar, 2017; Celauro et al., 2015; Komatsu, 2009; Wirtgen Group, 2022). Finally, the considered cost of aggregates has been 35 EUR/t.

4. Results and discussion

4.1. Repeated load triaxial test

The following subsections discuss the results obtained by testing the stabilized specimens dried before and after the exposure to 10 FT cycles. In addition, the mechanical response of the unstabilized UGM before FT cycles is also illustrated for comparison purposes and reported in dotted grey line in Figs. 8 and 10. The testing of UGM samples after FT cycles was out of the scope of this study. However, any possible damage on the rock aggregates due to freezing and thawing was very unlikely as the employed UGM is characterized by high resistance to FT actions as reported in section 2.

4.1.1. Resilient modulus

The experimental values of resilient moduli M_R and the corresponding trends estimated according to Hicks & Monismith model are reported for each stabilization treatment and for each tested sample in Fig. 7a and b considering before and after FT, respectively. Before the exposure to FT cycles, all the technologies enhance the response of the geomaterials, but the stiffness of some of the stabilized samples significantly decrease after undergoing cyclic FT actions, agreeing well with previous findings (Bolander, 1999; Little et al., 2007; Zhang et al., 2016).

In this regard, M_R of calcium chloride salt SAL-A, bentonite BEN, lignosulfonate LIG, reduced sugar SUG, petroleum resin RES remarkably decrease after 10 FT cycles. After the FT repetitions, the performance of SAL-A, BEN, LIG and SUG treatments become the same as the response of unstabilized UGM specimens due to the high solubility of these stabilizers when exposed to water (Kestler, 2009; Muhammad and Siddiqua, 2022; Zhang et al., 2020). SAL-A and BEN offer the best stabilization effect in terms of increased elastic stiffness before exposure to FT cycles.

The samples treated with all the other technologies become stiffer after FT cycles. These gains in M_R are most likely associated with the aging and cementing properties of the binders over the six-month temporal gap between the two rounds of RLTTs, as described in subsection 3.1.1. A portion of the observed increases in M_R may also occur due to internal compression during FT cycles that may have produced changes in the aggregate skeleton. Anyway, this effect is likely to account for a very small part of the improvements (Liu et al., 2018; Rosa et al., 2017).

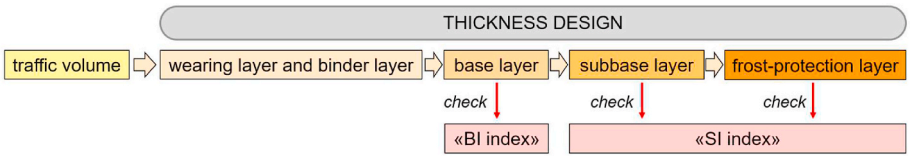

Fig. 5. Design workflow for a flexible pavement according to Norwegian pavement design code "N200" (NPRA, 2018, 2014).

Table 6
Traffic group category based on the number of equivalent 10-ton axles *N*.

Number of 10-ton axles N (· 10^5)	<5	5–10	10–20	20–35	35–100	>100
Traffic group	A	B	C	D	E	F

For the cement treated specimens, SAL-B shows a beneficial effect both before and after FT as the relationship $M_{R,\ SAL\text{-}B} > M_{R,\ CEM} > M_R$ is valid in both the cases.

While there are several works documenting the stiffness increase due to curing and aging of cement and bitumen treated geomaterials (Kim et al., 2002a, 2002b; Lu and Isacsson, 2002; Xuan et al., 2012), there are currently very few studies reporting on the long-term behavior of polymeric stabilization. In this regard, the very few previous laboratory investigations documented an increase in the compressive strength measured after 7 days and 28 days of curing (Newman et al., 2005; Santoni et al., 2002, 2005). Therefore, the results of this study indicate that the stabilization effects achieved with polyurethane POL, acrylate ACR, styrene butadiene STB, acetates ACE-A and ACE-B are not impaired by freezing-thawing actions. On the contrary, the obtained experimental data and their regression trends seem to buttress the hypothesis that an aging effect occurs and enhances the specimen's stiffness. Regarding the polymeric technologies, a significant amount of research has delved into the use of polyurethane POL to replace traditional bituminous binder for surface layers. Some studies highlighted a degradation in the mechanical response after FT cycles, but a fine gradation was selected for the tested samples (Chen et al., 2018; Cong et al., 2020). However, additional research is surely needed to address and understand the temporal development of the mechanical properties of aggregates stabilized with polymeric products. Finally, FT actions are not detrimental to the samples stabilized with synthetic fluid SF, agreeing well with previous findings (Gullu and Hazirbaba, 2010; Hazirbaba and Gullu, 2010).

Although the outcomes highlight some variation in the resilient behavior belonging to the two replicate specimens, the average results are calculated and reported in Fig. 8 without claiming to be exhaustive to hint at the overall changes in resilient behavior and compare them. In this regard, Table 8 specifies the values of the regression parameters k_1 and k_2. Future research should comprise the testing of at least three replicates to obtain more experimental data and thus reduce the statistical uncertainty.

4.1.2. Resistance to permanent deformation

The experimental data of accumulated plastic axial deformation $\varepsilon_{pl,a}$ and the corresponding trends assessed using Hyde model for both the tested specimens are illustrated in Fig. 9a and b referring to before and after the exposure to FT actions, respectively.

Overall, the obtained general trends agree with the outcomes found for the resilient modulus M_R. After the freezing-thawing actions the stabilization effect is considerably reduced for chloride salt SAL-A, bentonite BEN, lignosulfonate LIG, reduced sugar SUG. The performance of petroleum resin RES is also negatively affected by the FT cycles, albeit to a smaller extent.

As for the traditional stabilization technologies, only sample number 2 of cement CEM shows a certain degree of damage due to the FT cycles. The specimens containing bitumen BIT or a combination of cement and minerals mixture SAL-B display a better resistance against permanent deformation. This effect is likely due to curing and aging (Kim et al., 2002a, 2002b; Lu and Isacsson, 2002; Xuan et al., 2012). Considering the nontraditional stabilizers, the experimental results and modelled trends referring to almost all the polymer-based agents, namely polyurethane POL, acrylate ACR, styrene butadiene STB, acetate ACE-A, demonstrate a significant improvement in the permanent deformation properties. This phenomenon does not appear to be coincidental and can be connected with the gain in elastic stiffness due to the possible aging effect speculated and discussed in subsection 4.1.1 (Newman et al., 2005; Santoni et al., 2002, 2005). In this regard, polyurethane POL exhibits the most significant variation. Initially, the polyurethane POL stabilized materials attain the worst permanent deformation properties among all tested products (even poorer than UGM). Eventually, their mechanical response significantly improves over time as recorded in the second round of testing after FT cycles. The results indicate that acetate ACE-A produces the smallest permanent deformations among all the stabilizers. The specimen number 2 of acetate ACE-B does not exhibit an improved response during the second round of testing; therefore, future research should investigate more samples to better ascertain the associated deformation behavior. Anyway, the response of both the specimens stabilized with acetate ACE-B is better than the behavior of unstabilized UGM in both the rounds of testing.

Similarly to the considerations presented in subsection 4.1.1, the average results obtained from the testing of the two samples for each stabilization treatment are calculated and shown in Fig. 10. These experimental outcomes, without claiming to be exhaustive, give valuable indicative information regarding the overall behavioral trends despite the uncertainty stemming from the laboratory testing. Anyway, as already pointed out, future test programs should encompass at least three replicates to obtain a wider experimental dataset and thus decrease the statistical uncertainty. The average regression coefficient $\overline{a}_{HY}$ defining the average accumulated plastic axial deformation $\overline{\varepsilon}_{pl,a}$ is

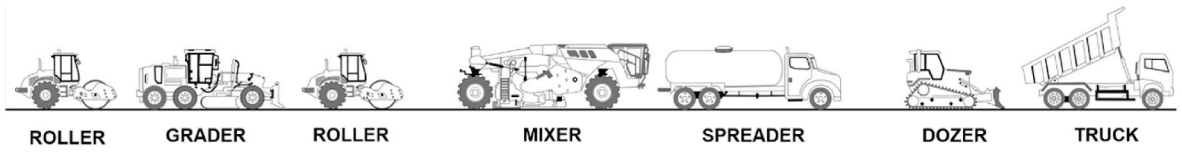

Fig. 6. Earthwork machines considered for the construction of a stabilized road base layer.

Table 7
Main characteristics of the earthwork machines.

	Capacity		Productivity (m^3/h)	Power (kW)	Fuel consumption			Cost
	(m)	(m^3)			(l/h)	(l/km)	(kg/kWh)	(EUR/h)
Truck	/	13.0	/	/	/	0.25	/	200
Dozer	4.0	/	200	150	/	/	0.25	250
Spreader	2.0	/	150	/	2	/	/	250
Mixer	2.0	/	200	/	70	/	/	450
Roller	1.8	/	500	/	40	/	/	200
Grader	4.0	/	2000	/	40	/	/	200

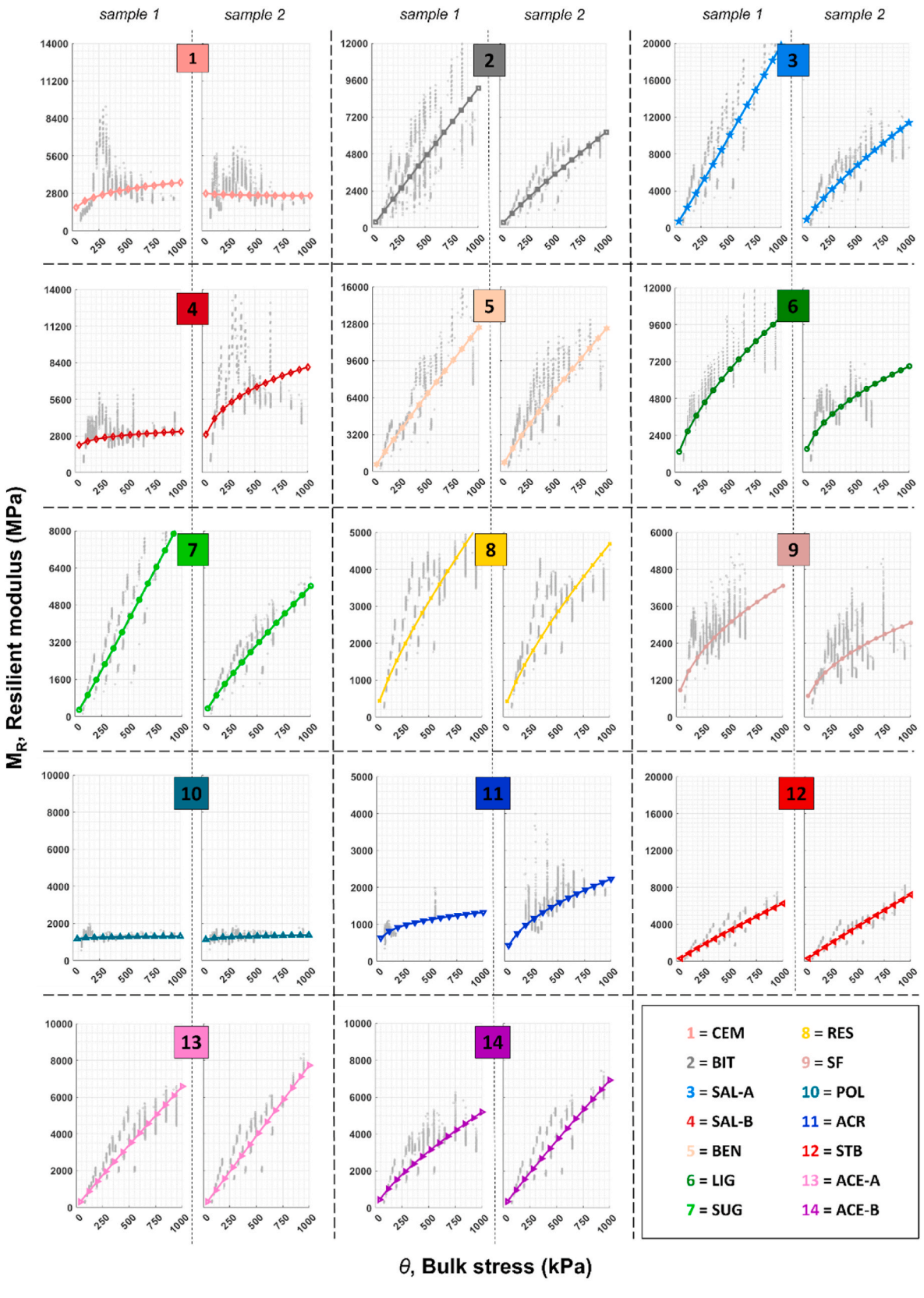

(a)

Fig. 7. Experimental data of resilient modulus M_R (grey dots) and calculated trends (colored solid lines) before (a) and after (b) 10 FT cycles.

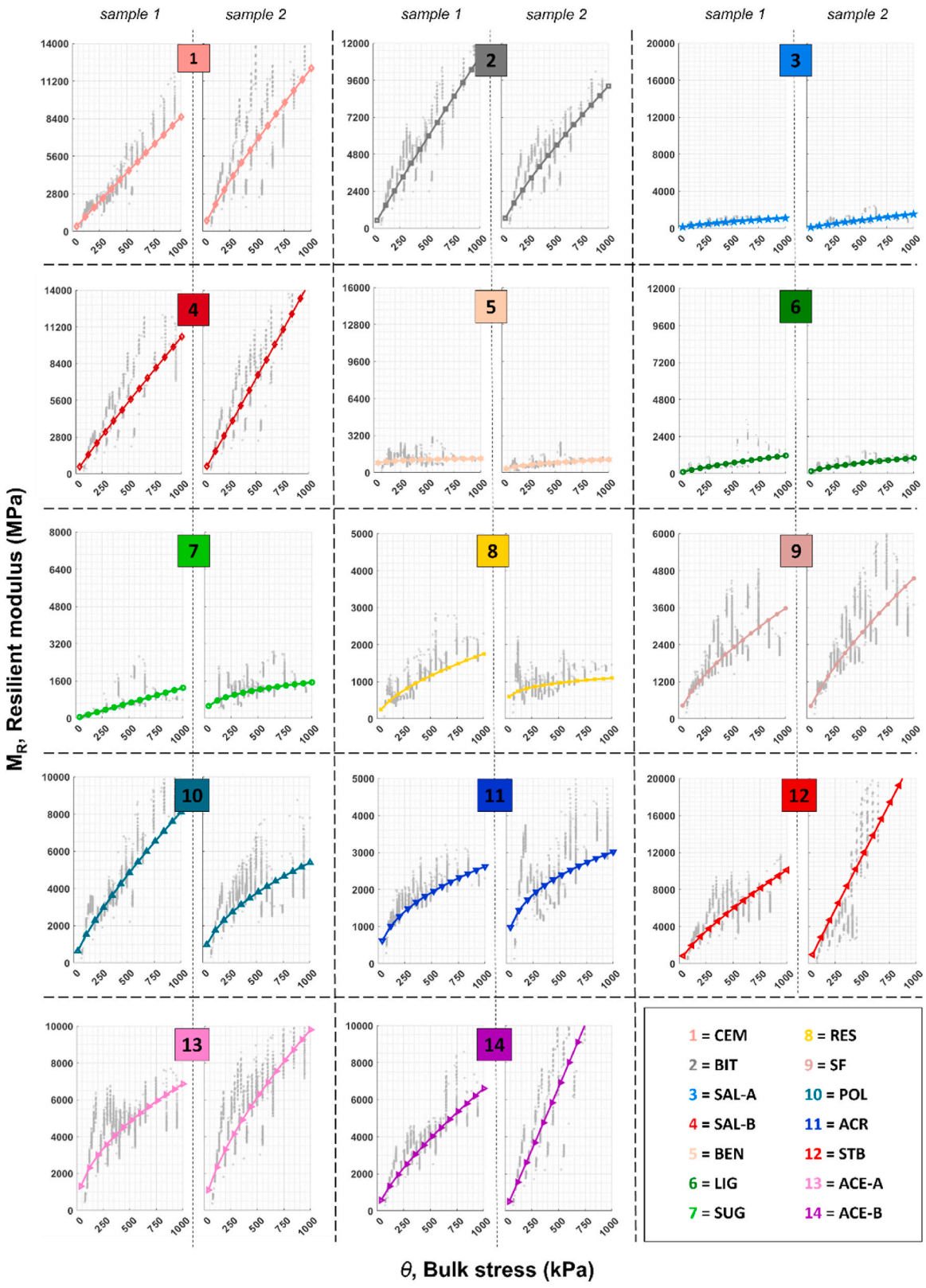

(b)

Fig. 7. (*continued*).

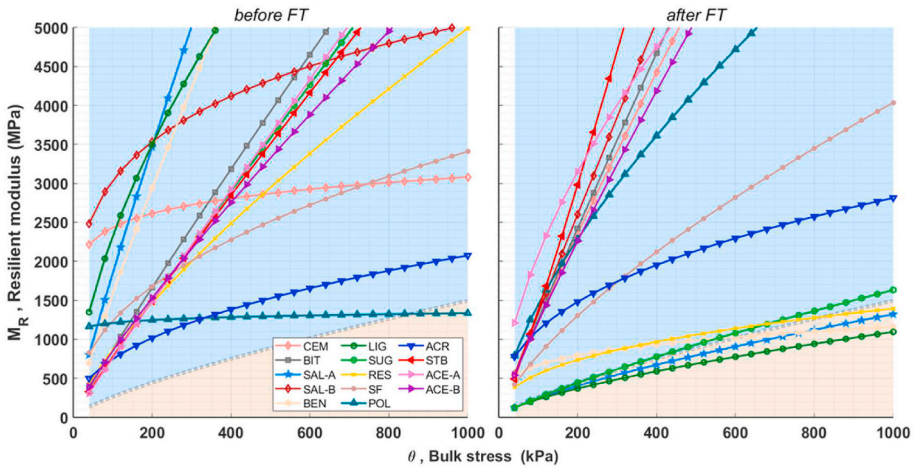

Fig. 8. Comparison between the trends of resilient moduli M_R before and after 10 FT cycles. The areas below and above the dotted grey line corresponding to UGM response are shaded as brown and blue, respectively.

computed as the mean of the five regression parameters a_{HY} pertaining to as many RLTT loading sequences. The values of $\bar{a}_{HY}$ calculated for both before and after the FT cycles are listed in Table 9.

As apparent in Fig. 10, the responses of the specimens stabilized with SAL-A, bentonite BEN, lignosulfonate LIG, reduced sugar SUG, resin RES are worse than those of untreated UGM samples. This finding can be explained considering that the permanent deformation behavior significantly varies with the tested aggregate gradation (Lekarp et al., 2000b). In this regard, the change in grading curve of the tested materials is due to the loss of fine particles occurring at the bottom and top ends of the specimens during the FT cycles as illustrated in Fig. 3.

The permanent deformation results can also be interpreted according to the Coulomb approach. Fig. 11 displays the percentages of the 30 loading steps composing each RLTT classified according to range A (plastic shakedown), range B (plastic creep) and range C (incremental collapse) averaged for each set of sample duplicates. In very good agreement with the findings derived by using the Hyde model, chloride salt SAL-A, bentonite BEN, lignosulfonate LIG, reduced sugar SUG and petroleum resin RES display a remarkable decrease in their performance after FT cycles. Chloride salt SAL-A produces the worst result. On the other hand, the Coulomb approach highlights that the most significant gains are associated with bitumen BIT and polyurethane POL. The responses pertaining to cement CEM, cement added minerals mixture SAL-B, acetates ACE-A and ACE-B are very similar or unvaried before and after the freezing-thawing actions, whereas the performance associated with acrylate ACR and styrene butadiene STB is slightly improved.

Table 8
Values of k_1 and k_2 parameters for Hicks & Monismith regression model.

	before FT cycles		after FT cycles	
	k_1	k_2	k_1	k_2
UGM	2637	0.75	/	/
CEM	24 350	0.10	12 528	0.91
BIT	8693	0.94	12 550	0.95
SAL-A	18 448	0.91	2426	0.74
SAL-B[a]	30 345	0.22	13 314	0.97
BEN	15 803	0.90	6727	0.24
LIG	23 212	0.59	2315	0.67
SUG	7723	0.95	2527	0.81
RES	8653	0.76	5578	0.40
SF	12 364	0.44	7994	0.70
POL	12 100	0.04	14 472	0.66
ACR	7480	0.44	11 222	0.40
STB	7766	0.94	13 713	1.12
ACE-A	7564	0.97	20 857	0.59
ACE-B	8506	0.85	12 199	0.90

[a] *Used in addition to CEM.*

4.1.3. Visual appearance of specimens surface

The surface appearance of the RLTT specimens tested both before and after 10 FT cycles is reported in Fig. 12. Furthermore, a microscope operating at a magnification of 40× was used to scrutinize the surface of small rock aggregates (dimension 8–11.2 mm), which also underwent 10 FT cycles according to the same procedure undertaken for RLTT samples.

The stabilizers calcium chloride salt SAL-A, bentonite BEN, lignosulfonate LIG, reduced sugar SUG completely disappear after the immersion of the samples in water and exposure to the freezing-thawing actions (Kestler, 2009; Muhammad and Siddiqua, 2022; Zhang et al., 2020). This entails the drastic changes in resilient modulus and resistance against permanent deformation of the corresponding specimens tested after 10 FT cycles: as already discussed in subsections 4.1.1 and 4.1.2, their response becomes the same of UGM when the stabilizer does not cover and bind the aggregate particles anymore. In this case, after the exposure to FT actions, it is possible to observe the main minerals composing the rock aggregates, e.g. amphibole, plagioclase and zoisite (Barbieri et al., 2019).

The appearance of the samples coated by all the other stabilizers look similar both before and the after the exposure to 10 FT cycles. The surfaces of the specimens treated with polyurethane POL, acrylate ACR, styrene butadiene STB, acetates ACE-A and ACE-B, albeit displaying the same spherical formations generated during the natural foaming, become opaquer after the six-month span between the first and second round of triaxial testing. The change in color of roads sealed with asphalt concrete (becomes clearer with time) or cement concrete (darkens with time) testifies aging of the binders (Kim et al., 2002a, 2002b; Lu and Isacsson, 2002; Xuan et al., 2012); in the same way, the modification in the color of polymeric binders may also be regarded as a visual occurrence proof of possible aging.

4.2. Design of stabilized road base layers

As defined by Equation (6), the load distribution coefficients a are assessed referring to the resilient modulus E_{200} expressed according to the Hicks & Monismith model for a bulk stress $\theta = 200$ kPa. The moduli regarded as inputs in Equation (6) are conveniently selected to make a conservative estimate in light of all the test results obtained both before and after FT actions. Therefore, the stiffness E_{200} of the specimens treated with cement CEM, bitumen BIT, cement and minerals mixture SAL-B, polyurethane POL, acrylate ACR, styrene butadiene STB, acetates ACE-A and ACE-B refer to the first round of RLTTs, namely before FT

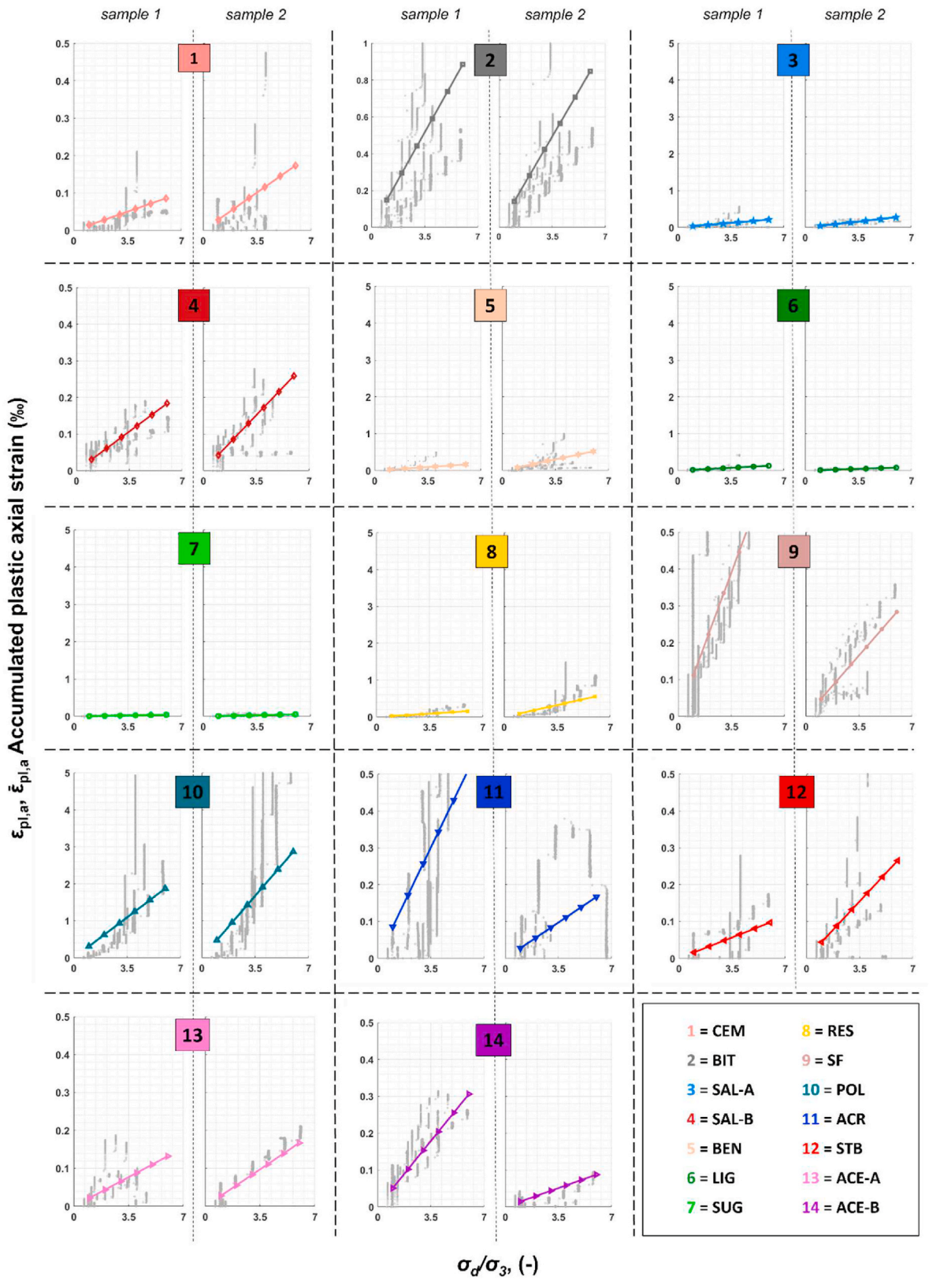

(a)

Fig. 9. Experimental data of accumulated plastic axial strain $\varepsilon_{pl,a}$ (grey dots) and average calculated trends $\bar{\varepsilon}_{pl,a}$ (colored solid lines) before (a) and after (b) 10 FT cycles.

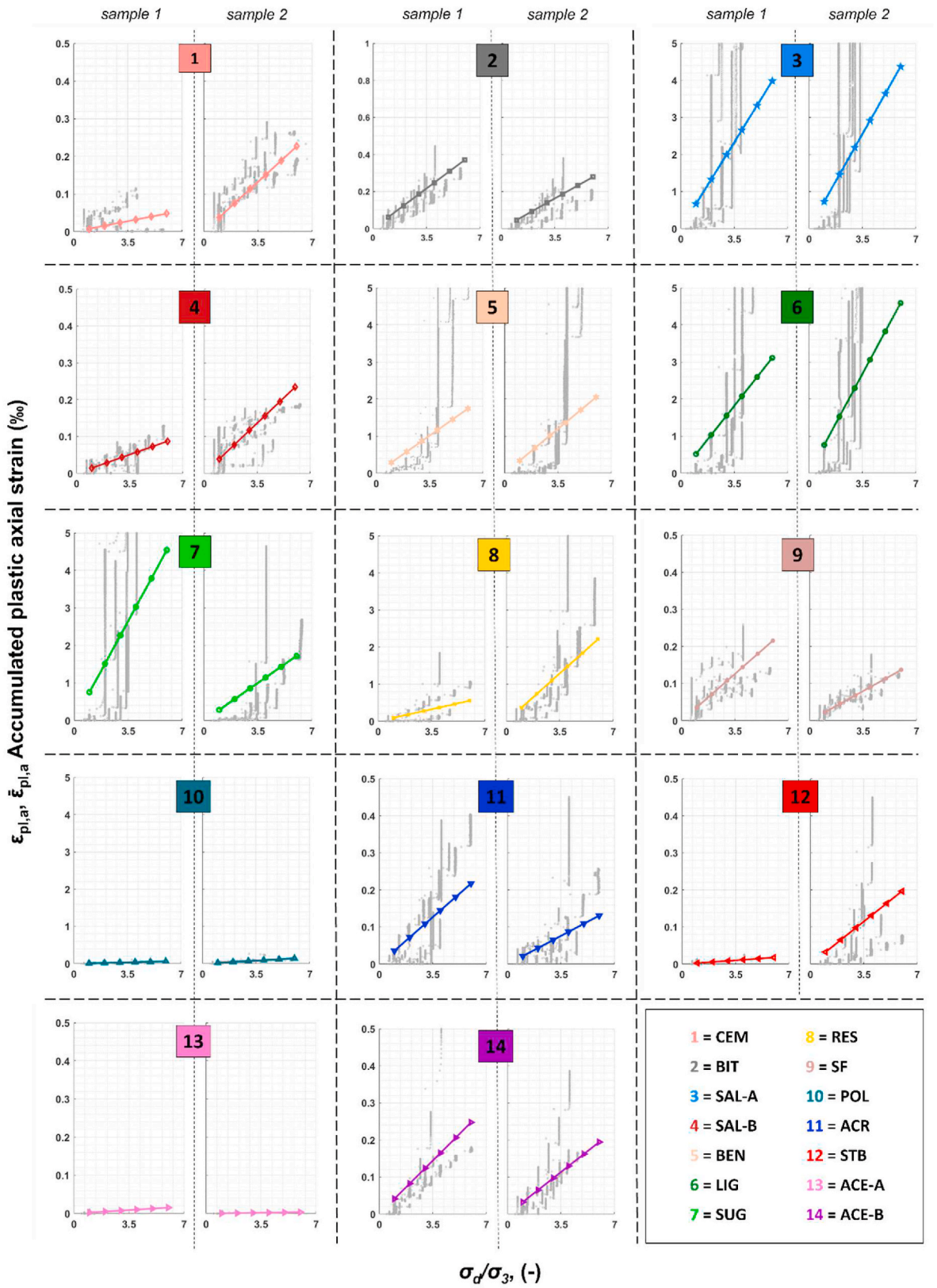

(b)

Fig. 9. (*continued*).

Table 9
Values of $\bar{a}_{HY}$ parameter for Hyde regression model.

	before FT cycles	after FT cycles
	$\bar{a}_{HY}$	$\bar{a}_{HY}$
UGM	0.165	/
CEM	0.020	0.037
BIT	0.144	0.054
SAL-A	0.041	0.618
SAL-B[a]	0.037	0.029
BEN	0.064	0.315
LIG	0.022	0.497
SUG	0.009	0.270
RES	0.074	0.240
SF	0.079	0.029
POL	0.387	0.021
ACR	0.065	0.031
STB	0.039	0.029
ACE-A	0.027	0.003
ACE-B	0.052	0.038

[a] *Used in addition to CEM.*

cycles, thus overlooking the observed improvements in mechanical response (possible aging).

Even though the organic non-petroleum and organic petroleum products show high sensitivity to water, their applications as potential road stabilizers are however taken into consideration for assessing the associated base thickness reduction. In this regard, field and laboratory experiences have demonstrated a satisfactory performance of these solutions, even when the stabilized road surfaces have been completely exposed to natural actions (Barbieri et al., 2021b; Onyejekwe and Ghataora, 2015; Tingle et al., 2007). However, it is highly recommended that lignosulfonate LIG, reduced sugar SUG, petroleum resin RES are applied in areas with no exposure to water. For instance, this can be ensured by incorporating a proper drainage system (e.g., well-maintained ditches and good crowning) or employing these stabilizers in dry regions (e.g., deserts and steppes). In this study, the resilient modulus E_{200} for the specimens treated with organic non-petroleum and organic petroleum products is conservatively estimated as the average of the two values E_{200} derived from the first and the second round of cyclic triaxial testing.

Finally, calcium chloride salt SAL-A and bentonite BEN are not taken into consideration. Referring to the published documents on their application on unpaved roads, these products are mostly used for dust control and fines preservation (Bergeson and Brocka, 1996; Gulia et al., 2019; Jones, 1999; Parsakhoo et al., 2020). Due to their high solubility, brine salt SAL-A and bentonite BEN do not provide sufficient long-term durable strength improvements and therefore would require very frequent rejuvenation operations.

The load distribution coefficients a calculated for the road base course stabilized with the considered types of technologies are listed in Table 10. Since a traditional unbound UGM road base is 20 cm thick, all the investigated solutions allow a significant reduction in base layer thickness by an average value of 10 cm. The most remarkable decrease (12.5 cm) is attained by the application of cement CEM and minerals mixture SAL-B, while the smallest thickness reduction (8.5 cm) is associated with reduced sugar SUG and acrylate ACR.

4.3. Assessment of carbon dioxide emissions and construction costs

In addition to the thickness reduction of the road base layer, the stabilization produces environmental benefits and cost savings. The amount of CO_2 generated during the construction of 1 km of the stabilized course as a function of the transport distance *TD* of aggregates is depicted in Fig. 13. The trend of the carbon dioxide emissions related to a traditional UGM base layer is highlighted with grey line (increase in $CDE/TD = 0.159$ t/km). In agreement with the considerations presented in section 4.2, the carbon footprints generated during the construction of a stabilized base layer are reduced by 50% on average. The most and least remarkable beneficial impacts are related to minerals mixture SAL-B (increase in $CDE/TD = 0.059$ t/km) and reduced sugar SUG (increase in $CDE/TD = 0.089$ t/km), respectively.

The *CDE* estimates based upon the construction operations and the transport of the rock aggregates are reported in Table 11. The former variable remains constant regardless *TD*, whereas the latter variable is linearly dependent on *TD* and is thus responsible for the increase in generated pollution. The beneficial effects highlighted in this study are generally in line with previous findings documenting the environmental implications of road stabilizers (Balaguera et al., 2018; Buritatum et al., 2021; van der Merwe Steyn and Visser, 2011).

Future research needs to estimate the carbon footprints also including the material procurement stage (i.e., production of each additive technology) using the "PRD" worksheet of the "HERMES CO_2" spreadsheet. In this regard, the Environmental Product Declaration (EPD) of every stabilizer technology must be considered. In this study, only the producer of lignosulfonate LIG was able to offer the corresponding EPD, whereas the manufacturers of all the other nontraditional technologies could not provide EPDs or similar documentation, either because they have not yet been created or are confidential. Although the material procurement stage cannot be addressed here, the evaluation of CO_2 emissions for the construction stage performed in this study already represents a new relevant contribution as highlighted in Table 2.

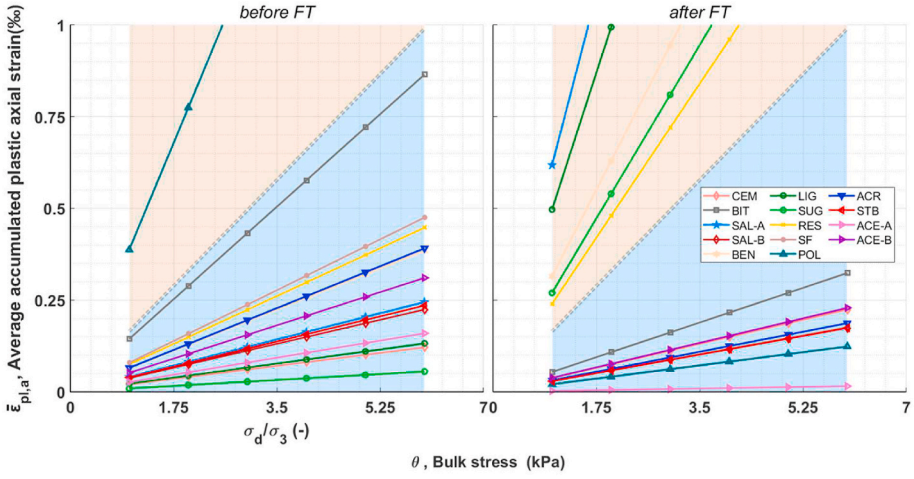

Fig. 10. Comparison between the average trends of accumulated plastic axial strain $\bar{\varepsilon}_{pl,a}$ before and after 10 FT cycles. The areas above and below the dotted grey line corresponding to UGM response are shaded as brown and blue, respectively.

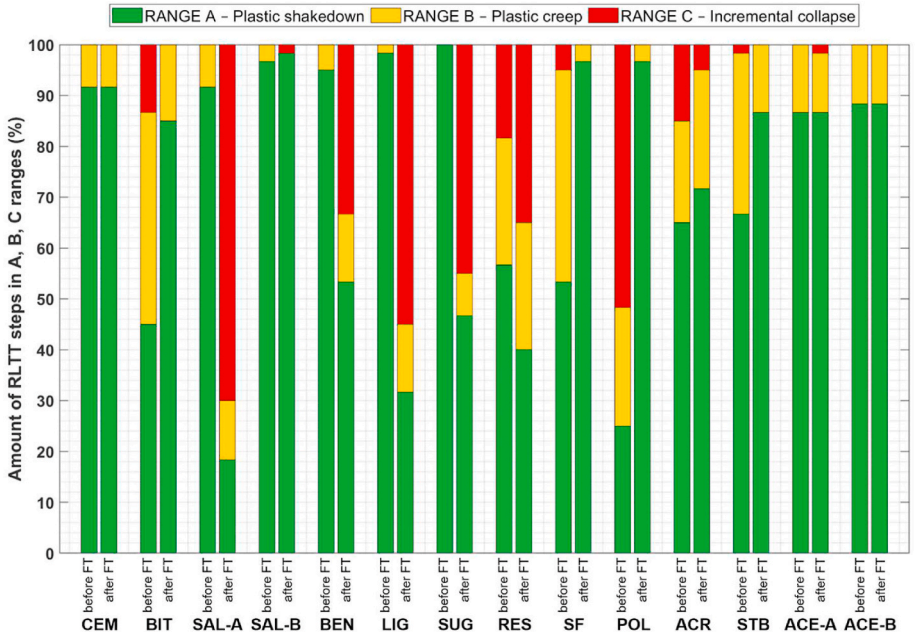

Fig. 11. Classification of each RLTT step based on the permanent deformations measured before and after FT cycles.

From an economic perspective, it is necessary to assess the convenience of applying each different stabilizer compared to laying a traditional untreated UGM base. In this regard, Fig. 14 shows the construction cost as a function of the transport distance *TD* of the aggregates. The application of most of the tested technologies is always convenient, whereas *TD* becomes a crucial factor to determine the economic competitiveness of a few stabilizers. Critical transport distance TD_{cr} is defined as the mileage above which the creation of a stabilized base course is cheaper than a traditional unstabilized one. This parameter can help practitioners decide when individual stabilization alternatives are cost-effective. The calculated TD_{cr} for reduced sugar SUG, synthetic fluid SF, styrene butadiene STB, acetates ACE-A and ACE-B are 17 km, 28 km, 64 km, 80 km and 66 km, respectively. The application of polyurethane POL is particularly expensive with TD_{cr} = 253 km. The price to realize a traditional UGM base layer is highlighted with grey line (1152 EUR per km of *TD*). Considering stabilized base courses, the application of cement CEM with minerals mixture SAL-B is characterized by the lowest cost increase (432 EUR per km of *TD*), while the stabilization with reduced sugar SUG produces the highest increase (662 EUR per km of *TD*).

Fig. 15 disaggregates the total costs considering all the expenditures necessary for the realization of a stabilized base layer (aggregates supply, stabilizer supply, fieldwork activities, aggregates transport) for different values of *TD*. The price of the selected stabilizer is determining to assess the overall cost of the construction operations. Stabilization of the UGM base layer with reduced sugar SUG, petroleum resin RES, synthetic fluid SF, polyurethane POL, styrene butadiene STB, acetates ACE-A and ACE-B is more expensive than the application of the traditional solutions, namely cement CEM and bitumen BIT, for any values of *TD*. The use of lignosulfonate LIG or acrylate ACR is cheaper than cement CEM and bitumen BIT only for a certain range of *TD*. As also reported in previous studies (Bushman et al., 2005; Khoeini et al., 2019; Uys et al., 2011), the application of several polymer-based products is usually at the higher end of the pricing scale and this is mainly due to low-scale production, expensive raw materials and current sales system (Huang et al., 2021). To better characterize the economic viability of each stabilization technology, further research should estimate the life-cycle costs including maintenance costs. In this regard, to fully characterize the long-term behavior of the stabilized materials and develop accurate predictions for required maintenance cycles, more laboratory and field tests are needed.

5. Conclusions

Considering the extent of unbound layers forming the global road network and the subsequent need for effective construction and maintenance operations, stabilization technologies represent attractive solutions to comply with the target mechanical performance. Currently there are many commercially available stabilizers, while the relative maturity and understanding of these products in terms of performance, economic and environmental perspectives are in their infancy.

Therefore, this research has focused on achieving a systematic comparison encompassing all the existing categories of products which are reportedly able to stabilize the coarse-graded materials that are typically used in road base layers. The stabilization potential of the selected technologies for improving the mechanical properties of coarse aggregate samples has been assessed via Repeated Load Triaxial Test (RLTT). Their elastic stiffness and deformation properties have been evaluated both before and after the exposure to 10 Freeze-Thaw (FT) cycles. The time span between the first and the second round of testing, namely before and after FT cycles, was 6 months. Conservative results have been used to evaluate the thickness reduction of stabilized base layers as compared to an untreated UGM base layer for a road pavement built in Norway. Finally, estimates of the carbon dioxide emissions as well as the economic costs pertaining to the construction of unstabilized and stabilized base courses have been appraised using the "HERMES CO_2" spreadsheet tool. Chloride salt SAL-A and bentonite BEN have not been considered in these environmental and economic assessments due to their very high sensitivity to water exposure. It is highly recommended that aggregates stabilized with lignosulfonate LIG, reduced sugar SUG, petroleum resin RES should not be used where exposure to water is likely to occur. Thus, the application of these stabilizers should be limited to dry regions and/or complemented with proper drainage designs and practices to achieve a satisfactory performance.

Table 12 reports a concise comparison of the main findings for each investigated stabilizing agent. The following conclusions can be drawn:

(1) Specimens stabilized with cement CEM, combination of cement and minerals mixture SAL-B, bitumen BIT, synthetic fluid SF, polyurethane POL, acrylate ACR, styrene butadiene STB, acetates

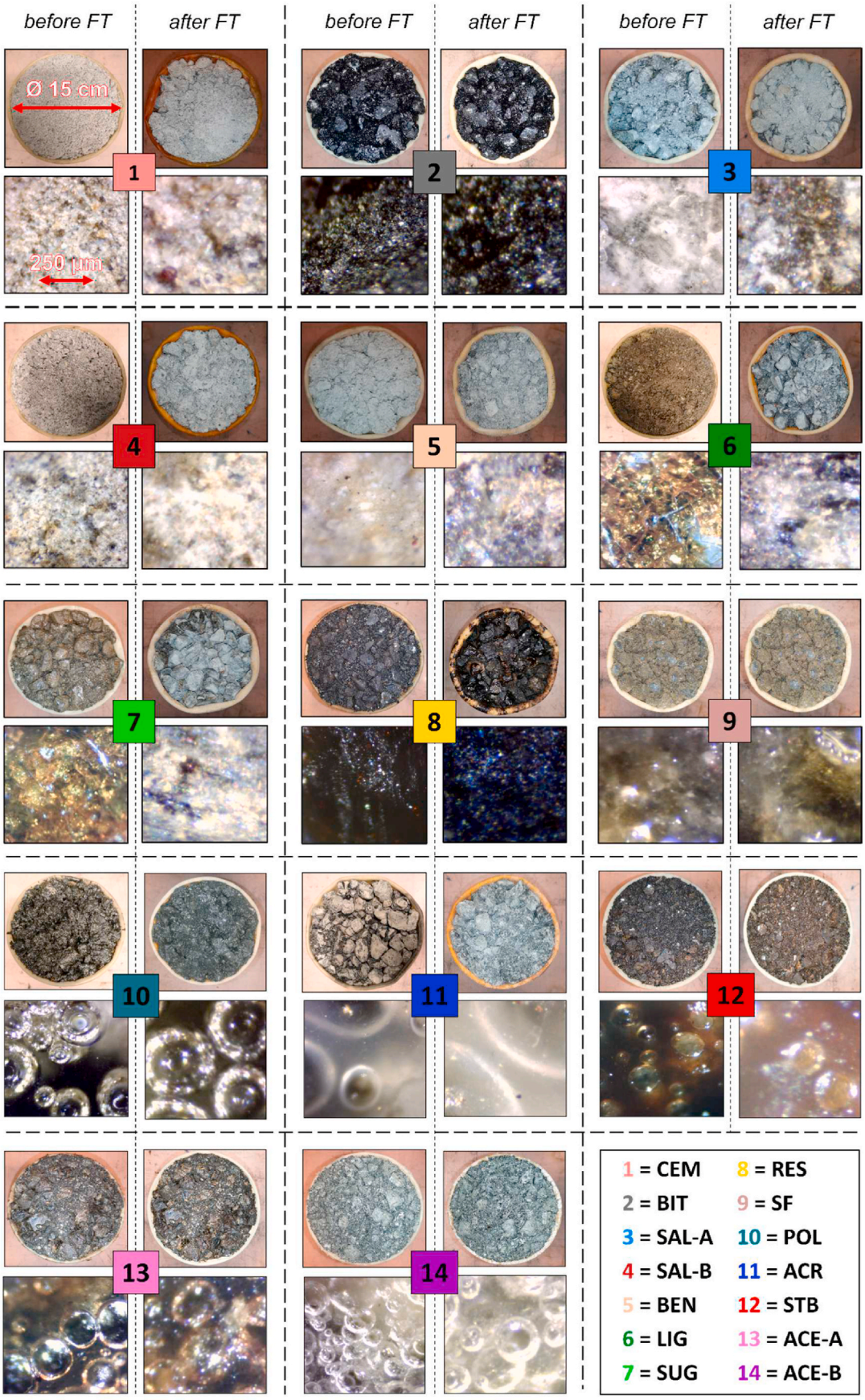

Fig. 12. Appearance of stabilized RLTT samples and aggregates before and after 10 FT cycles.

Table 10
Values of load distribution coefficients a and thickness of road base layers for different stabilization treatments.

Technology	E_{200}	a	Thickness of stabilized base	Thickness reduction compared to UGM base[a]
	(kPa)	(–)	(cm)	(cm)
CEM	2614	2.10[d]	8.5	11.5
BIT	1664	2.00	10.0	10.0
SAL-B[b]	3535	2.10[d]	7.5	12.5
LIG[c]	1936	2.10	9.5	10.5
SUG[c]	969	1.70	11.5	8.5
RES[c]	1101	1.75	11.0	9.0
SF	1302	1.85	10.5	9.5
POL	1246	1.85	10.5	9.5
ACR	1017	1.70	11.5	8.5
STB	1487	1.95	10.0	10.0
ACE-A	1486	1.95	10.0	10.0
ACE-B	1530	1.95	10.0	10.0

[a] Thickness of UGM base is 20 cm.
[b] Used in addition to CEM.
[c] Good stabilization with no exposure to water (e.g., proper drainage system, dry regions).
[d] Maximum allowable value (subsection 3.2).

ACE-A and ACE-B show improved mechanical performance both before and after the exposure to 10 FT cycles. These stabilizers display good freezing durability. Moreover, their mechanical properties seem to exhibit a time-dependent improvement (possible aging effect).

(2) Due to their high solubility in water, the mechanical performance of specimens stabilized with calcium chloride salt SAL-A, bentonite BEN, lignosulfonate LIG, reduced sugar SUG, petroleum resin RES significantly decrease after the exposure to 10 FT cycles.

(3) The studied stabilizers can significantly reduce the thickness of a traditional untreated base layer by an average value of 50%. This diminishes the amount of needed construction aggregates as well as lowers the related transport and construction costs.

(4) As a consequence of the reduced thickness of base course, all the stabilizers significantly lower the carbon dioxide emissions during the construction operations. Depending upon the selected product, the values of these reductions range from 44% to 63%.

(5) The construction cost of a treated base layer is significantly dependent upon the price of the selected stabilizer. Compared to a traditional UGM base course, the application of most of the studied technologies is more economic, whereas the transport distance *TD* of the aggregates is a crucial factor for the economic competitiveness of some stabilizers. In this regard, the higher cost of several polymer-based technologies hinders their use in favor of traditional solutions. However, it should be noted that these innovative technologies provide greater benefits in terms of mechanical properties in comparison with traditional stabilizers.

For future research, the following topics should be addressed for more comprehensive characterization and implementation:

Table 11
Generation of carbon dioxide emissions for 1 km of a stabilized road base layer.

Technology	CO_2 emission of construction	CO_2 emission of transport TD
	(t)	(t/km)
UGM	1.083	0.159
CEM	1.183	0.068
BIT	1.392	0.079
SAL-B[a]	1.044	0.059
LIG	1.322	0.074
SUG	1.600	0.089
RES	1.531	0.085
SF	1.461	0.081
POL	1.461	0.080
ACR	1.600	0.087
STB	1.392	0.075
ACE-A	1.392	0.075
ACE-B	1.392	0.074

[a] Used in addition to CEM.

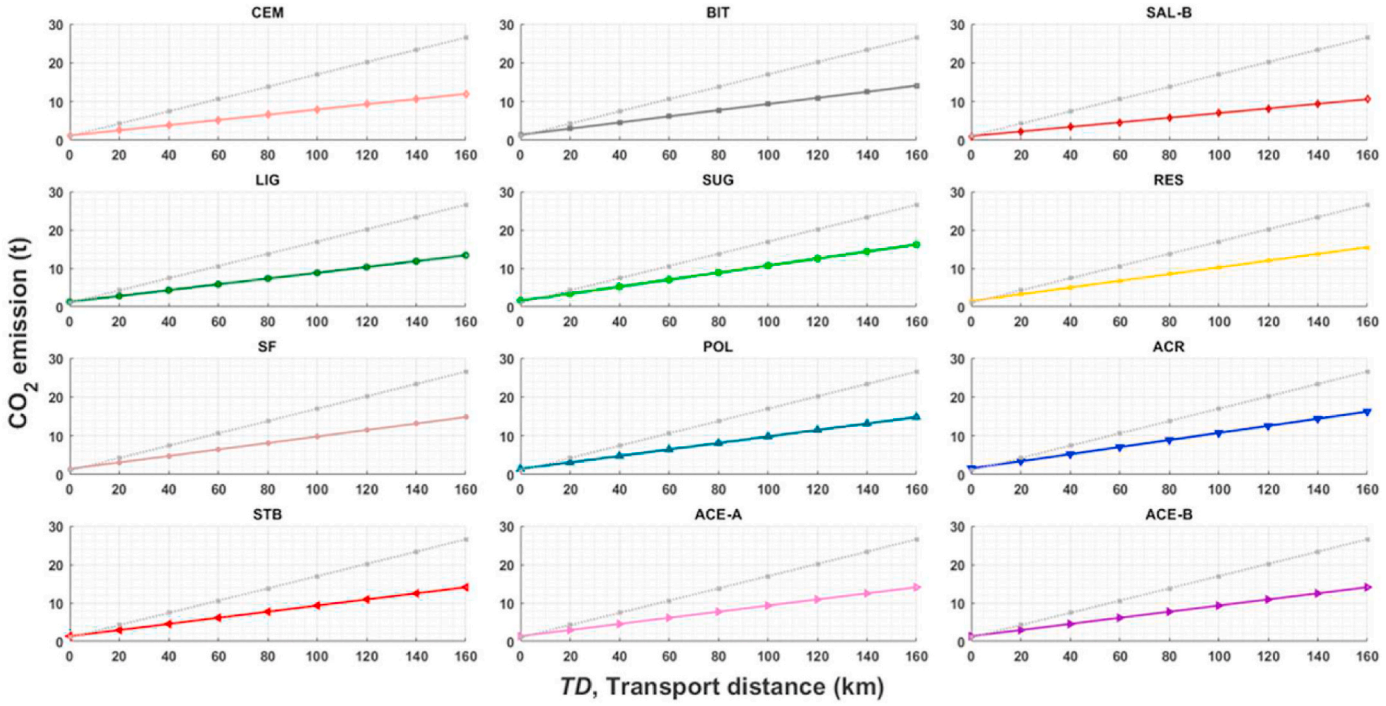

Fig. 13. Carbon dioxide emissions generated during construction of 1 km of a stabilized road base layer as a function of aggregates transport distance *TD* (compared to the construction of a traditional UGM base layer, grey line).

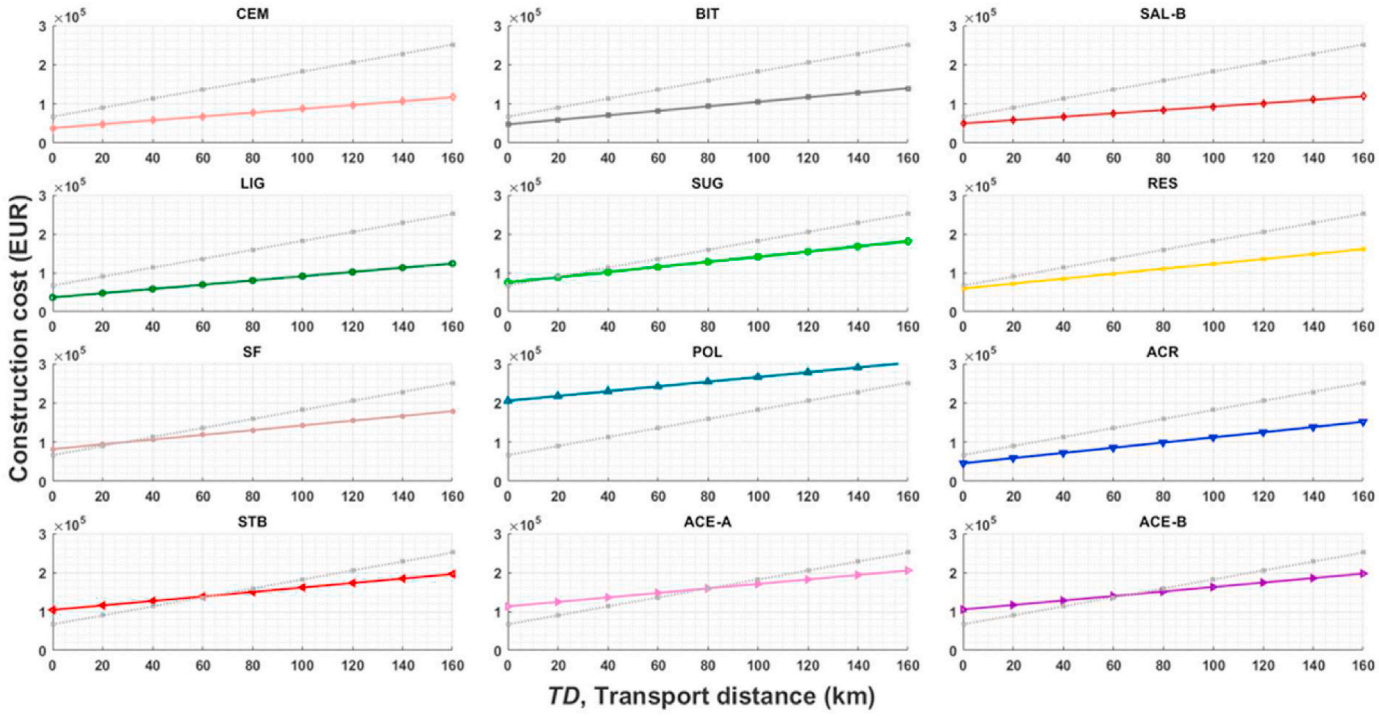

Fig. 14. Cost of construction of a stabilized road base layer of 1 km as a function of aggregates transport distance *TD* (compared to the construction of a traditional UGM base layer, grey line).

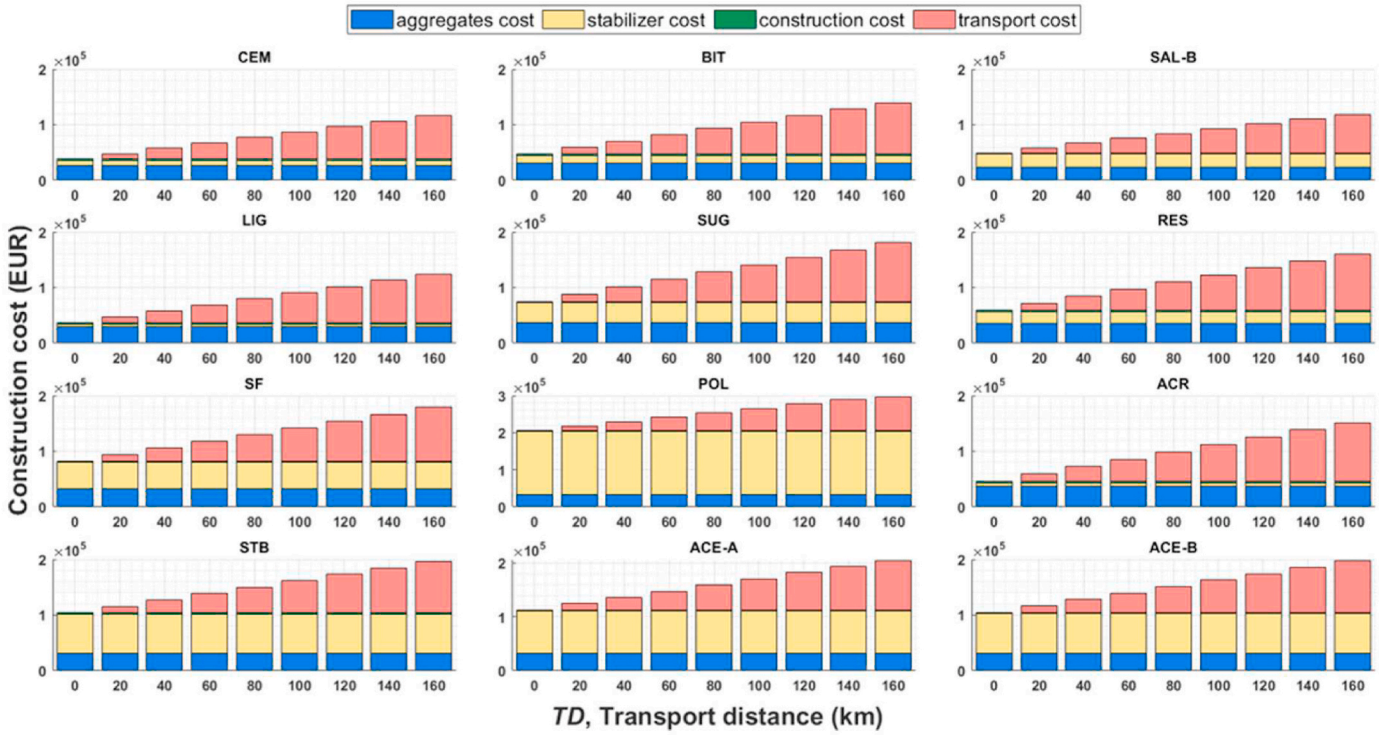

Fig. 15. Cost of construction for 1 km of a stabilized road base layer.

Table 12
Suitability assessment of the investigated stabilizers for coarse-graded aggregates; freeze-thaw durability and comparison with the construction of a traditional UGM base layer.

Stabilizer	Suitability assessment			
	Freeze-thaw durability	Thickness reduction	CO_2 emission reduction	Economically convenient TD[a]
Cement	High	−58%	−58%	any TD
Bitumen	High	−50%	−50%	any TD
Calcium chloride	Low	*not considered*	*not considered*	*not considered*
Minerals mixture[b]	High	−63%	−63%	any TD
Bentonite	Low	*not considered*	*not considered*	*not considered*
Lignosulfonate[c]	Low	−53%	−53%	any TD
Reduced sugar[c]	Low	−43%	−44%	TD > 17 km
Petroleum resin[c]	Low	−45%	−47%	any TD
Synthetic fluid	High	−48%	−49%	TD > 28 km
Polyurethane	High	−48%	−50%	TD > 253 km
Acrylate	High	−43%	−45%	any TD
Styrene butadiene	High	−50%	−53%	TD > 64 km
Acetate A	High	−50%	−53%	TD > 80 km
Acetate B	High	−50%	−53%	TD > 66 km

[a] Transport Distance (TD) of the aggregates.
[b] Used in addition to CEM.
[c] Good stabilization with no exposure to water (e.g., proper drainage system, dry regions).

(i) Appraisal of stiffness and strength of stabilized materials for various ranges of curing time, immersion time, temperature and humidity. Moreover, variations in grain size distribution, geological origin of rock aggregates and stabilizer content can also be considered. The number of RLTT replicate samples should be increased to three or more to reduce statistical uncertainty and better characterize those stabilization technologies which perform better than others.
(ii) Based on the results of (i), trial full-scale road sections could be constructed and their performance recorded to validate the laboratory test findings. The critical analysis of laboratory and field results would provide relevant inputs to develop road design guidelines and codes of practice for stabilization using nontraditional technologies.
(iii) Based on the outputs derived from (i) and (ii), it would be possible to estimate the frequency of the necessary maintenance operations. Furthermore, the public availability of EPDs for each stabilizer is needed to enable considerations also encompassing the material production phase. Eventually, more accurate life-cycle cost models could be developed to evaluate the pollution as well as the associated economic costs during the entire road lifespan.

CRediT authorship contribution statement

Diego Maria Barbieri: Conceptualization, Methodology, Software, Validation, Formal analysis, Investigation, Resources, Data curation, Writing – original draft, Visualization, Project administration. **Baowen Lou:** Conceptualization, Methodology, Software, Validation, Formal analysis, Investigation, Resources, Data curation, Writing – original draft. **Robert Jason Dyke:** Conceptualization, Methodology, Formal analysis, Investigation, Resources, Data curation, Writing – review & editing. **Xueting Wang:** Resources, Writing – review & editing, Visualization. **Hao Chen:** Investigation, Resources, Writing – review & editing, Visualization. **Benan Shu:** Resources, Writing – review & editing, Visualization. **Uneb Gazder:** Visualization, Supervision. **Suksun Horpibulsuk:** Writing – review & editing, Visualization, Supervision. **Jeb S. Tingle:** Writing – review & editing, Visualization, Supervision. **Inge Hoff:** Conceptualization, Methodology, Writing – review & editing, Visualization, Supervision, Project administration, Funding acquisition.

Declaration of competing interest

The authors declare that they have no known competing financial interests or personal relationships that could have appeared to influence the work reported in this paper.

Data availability

Data will be made available on request.

Acknowledgments

This paper is dedicated to the memory of Mrs. Elisabetta Maria Oesch and Mr. Flavio Barbieri. This work was supported by the Norwegian Public Roads Administration (VegDim project, grant number 605377) and by the Research Council of Norway (HERMES project, grant number 299538). The support kindly provided by the laboratory assistants Bent Lervik, Jan Erik Molde, Lisbeth Johansen, Frank Stæhli and Tage Westrum is greatly acknowledged. Aggregates kindly provided by Franzefoss Pukkverk avd. Vassfjell, Heimdal, Norway. Bitumen kindly supplied by Nynas AS, Drammen, Norway. Calcium chloride kindly supplied by TETRA Chemicals Europe AB, Helsingborg, Sweden. Minerals mixture (Good Road Soil Stabilizer GRSS) kindly supplied by InnoCSR Co. Ltd., Seoul, South Korea. Bentonite kindly provided by Imerys Metalcasting, Mannheim, Germany. Lignosulfonate (Dustex) kindly supplied by Borregaard AS, Sarpsborg, Norway. Reduced sugar (Dust Stop) kindly supplied by Cypher Environmental, Winnipeg, Canada and Vumos Corp., Kajaani, Finland. Petroleum resin (PennzSuppress) kindly supplied by PennzSuppress Corp., Bradford, USA. Polyurethane (Elastopave) kindly supplied by BASF, Lemförde, Germany. Acrylates (Soil Control) kindly supplied by Sparks AS, Asker, Norway, Evonik Industries, Essen, Germany and Alberdingk Boley, Krefeld, Germany. Synthetic fluid (SECUR 35), styrene butadiene (Eco-Pave H), acetate-A (Eco-Pave E) and acetate-B (Soil Sement Engineered formula 69PBc) kindly supplied by Midwest, Canton, USA. The above information regarding stabilizer trade names and their suppliers are reported for informational purposes only and the inclusion of this information does not imply endorsement of any product or company. The findings and opinions reported are those of the authors and not necessarily those of the stabilizer suppliers.

References

AASHTO, 1993. AASHTO Guide for Design of Pavement Structure. USA.
AASHTO, 1986. Standard Specifications for Transportation Materials and Methods of Sampling and Testing, Part II. USA.
Akbas, M., Iyisan, R., Dayioglu, A.Y., Hatipoglu, M., 2021. Stiffness properties of recycled concrete aggregates as unbound base and subbase materials under freeze and thaw cycles. Arabian J. Sci. Eng. 46, 10569–10584. https://doi.org/10.1007/s13369-021-05344-w.
Alnedawi, A., Nepal, K.P., Al-Ameri, R., 2019. New shakedown criterion and permanent deformation properties of unbound granular materials. J. Mod. Transp. 27, 108–119. https://doi.org/10.1007/s40534-019-0185-2.
Alnedawi, A., Ullah, S., Azam, A., Mousa, E., Obaid, I., Yosri, A., 2022. Integrated and holistic knowledge map of resilient modulus studies for pavement materials: a scientometric analysis and bibliometric review of research frontiers and prospects. Transp. Geotech. 33, 100711 https://doi.org/10.1016/j.trgeo.2021.100711.
Amran, Y.H.M., Alyousef, R., Alabduljabbar, H., El-Zeadani, M., 2020. Clean production and properties of geopolymer concrete; A review. J. Clean. Prod. 251, 119679 https://doi.org/10.1016/j.jclepro.2019.119679.
Araya, A., Molenaar, A.A.A., Houben, L.J.M., 2010. Characterization of unbound granular materials using repeated load CBR and triaxial testing. In: Huang, B., Tutumluer, E., Al-Qadi, I.L., Prozzi, J., Shu, X. (Eds.), GeoShanghai International Conference 2010. ASCE, Shanghai, pp. 355–363. https://doi.org/10.1061/41104(377)44.

Arulrajah, A., Baghban, H., Narsilio, G.A., Horpibulsuk, S., Leong, M., 2020. Discrete element analysis of recycled concrete aggregate responses during repeated load triaxial testing. Transp. Geotech. 23, 100356 https://doi.org/10.1016/j.trgeo.2020.100356.

Arulrajah, A., Piratheepan, J., Disfani, M.M., Bo, M.W., 2013. Geotechnical and geoenvironmental properties of recycled construction and demolition materials in pavement subbase applications. J. Mater. Civ. Eng. 25, 1077–1088 https://doi.org/10.1061/(ASCE)MT.1943-5533.0000652.

Aursand, P.O., Horvli, I., 2009. Effect of a changed climate on gravel roads. In: Tutumluer, E., Al-Qadi, I. (Eds.), Bearing Capacity of Roads, Railways and Airfields - Proceedings of the 8th International Conference on the Bearing Capacity of Roads, Railways and Airfields. Taylor & Francis, Urbana, pp. 1091–1099.

Balaguera, A., Carvajal, G.I., Albertí, J., Fullana-i-Palmer, P., 2018. Life cycle assessment of road construction alternative materials: a literature review. Resour. Conserv. Recycl. 132, 37–48. https://doi.org/10.1016/j.resconrec.2018.01.003.

Barbieri, D.M., Dorval, J.-G., Lou, B., Chen, H., Shu, B., Wang, F., Hoff, I., 2021a. Dataset regarding the mechanical characterization of sedimentary rocks derived from Svalbard for possible use in local road constructions. Data Brief 34, 106735. https://doi.org/10.1016/j.dib.2021.106735.

Barbieri, D.M., Hoff, I., Mork, H., 2017. Laboratory investigation on unbound materials used in a highway with premature damage. In: Loizos, A., Al-Qadi, I.L., Scarpas, A.T. (Eds.), 10th International Conference on the Bearing Capacity of Roads, Railways and Airfields. Taylor & Francis, Athens, pp. 101–108. https://doi.org/10.1201/9781315100333.

Barbieri, D.M., Hoff, I., Mørk, M.B.E., 2019. Mechanical assessment of crushed rocks rerived from tunnelling operations. In: Cheng, W.-C., Yang, J., Wang, J. (Eds.), Sustainable Civil Infrastructures. Springer, Hangzhou, pp. 225–241. https://doi.org/10.1007/978-3-319-95783-8_19.

Barbieri, D.M., Lou, B., Chen, H., Shu, B., Wang, F., Hoff, I., 2021b. Organosilane and lignosulfonate stabilization of roads unbound: performance during a two-year time span. Adv. Civ. Eng. 2021 https://doi.org/10.1155/2021/9367501.

Barbieri, D.M., Lou, B., Dyke, R.J., Chen, H., Wang, F., Connor, B., Hoff, I., 2022a. Mechanical properties of roads unbound treated with synthetic fluid based on isoalkane and tall oil. Transp. Geotech. 32, 100701 https://doi.org/10.1016/j.trgeo.2021.100701.

Barbieri, D.M., Lou, B., Dyke, R.J., Chen, H., Wang, F., Dongmo-Engeland, B., Tingle, J. S., Hoff, I., 2022b. Stabilization of coarse aggregates with traditional and nontraditional additives. J. Mater. Civ. Eng. 34 https://doi.org/10.1061/(ASCE)MT.1943-5533.0004406.

Barbieri, D.M., Lou, B., Wang, F., Hoff, I., Wu, S., Li, J., Vignisdottir, H.R., Bohne, R.A., Anastasio, S., Kristensen, T., 2021c. Assessment of carbon dioxide emissions during production, construction and use stages of asphalt pavements. Transp. Res. Interdiscip. Perspect. 11, 100436 https://doi.org/10.1016/j.trip.2021.100436.

Barnes, D., Ph, D., Connor, B., 2014. Alaska Soil Stabilization Guide 2014 Update. Fairbanks.

Bassani, M., Tefa, L., 2018. Compaction and freeze-thaw degradation assessment of recycled aggregates from unseparated construction and demolition waste. Construct. Build. Mater. 160, 180–195. https://doi.org/10.1016/j.conbuildmat.2017.11.052.

Beaulieu, L., Pleau, R., Pierre, P., Poulin, P., Juneau, S., 2014. Mechanical performance in field conditions of treated and stabilized granular materials used in unpaved roads: a longitudinal study. Can. J. Civ. Eng. 41, 97–105 https://doi.org/10.1139/cjce-2012-0423.

Bergeson, K.L., Brocka, S.G., 1996. Bentonite treatment for fugitive dust control. In: Sixth International Conference on Low-Volume Roads. National Academy Press, Minneapolis, pp. 261–271.

Blanck, G., Cuisinier, O., Masrouri, F., 2016. Life cycle assessment of non-traditional treatments for the valorisation of dry soils in earthworks. Int. J. Life Cycle Assess. 21, 1035–1048. https://doi.org/10.1007/s11367-016-1076-y.

Blanck, G., Cuisinier, O., Masrouri, F., 2014. Soil treatment with organic non-traditional additives for the improvement of earthworks. Acta Geotech 9, 1111–1122. https://doi.org/10.1007/s11440-013-0251-6.

Bolander, P., 1999. Laboratory testing of nontraditional additives for stabilization of roads and trail surfaces. Transp. Res. Rec. J. Transp. Res. Board 2, 24–31. https://doi.org/10.3141/1652-38.

Buritatum, A., Horpibulsuk, S., Udomchai, A., Suddeepong, A., Takaikaew, T., Vichitcholchai, N., Horpibulsuk, J., Arulrajah, A., 2021. Durability improvement of cement stabilized pavement base using natural rubber latex. Transp. Geotech. 28, 100518 https://doi.org/10.1016/j.trgeo.2021.100518.

Bushman, W.H., Freeman, T.E., Hoppe, E.J., 2005. Stabilization techniques for unpaved roads. Transp. Res. Rec. J. Transp. Res. Board 28–33. https://doi.org/10.1177/0361198105193600104, 1936.

Caterpillar, 2017. Caterpillar Performance Handbook. Peoria.

Celauro, C., Corriere, F., Guerrieri, M., Lo Casto, B., 2015. Environmentally appraising different pavement and construction scenarios: a comparative analysis for a typical local road. Transport. Res. Transport Environ. 34, 41–51. https://doi.org/10.1016/j.trd.2014.10.001.

CEN, 2022. ISO 17472 Sustainability of Construction Works. Sustainability Assessment Civil Engineering Works. Calculation methods, Belgium.

CEN, 2019a. ISO 15804 Sustainability of Construction Works. Environmental Product Declarations. Core Rules for the Product Category of Construction Products. Belgium.

CEN, 2019b. ISO 13242 Aggregates for Unbound and Hydraulically Bound Materials for Use in Civil Engineering Work and Road Construction. Belgium.

CEN, 2011. ISO 1097-1 Tests for Mechanical and Physical Properties of Aggregates. Part 1: Determination of the Resistance to Wear (Micro-deval). Belgium.

CEN, 2010. ISO 1097-2 Tests for Mechanical and Physical Properties of Aggregates. Part 2: Methods for the Determination of Resistance to Fragmentation. Belgium.

CEN, 2007. ISO 1367-1 Tests for Thermal and Weathering Properties of Aggregates. Part 1: Determination of Resistance to Freezing and Thawing. Belgium.

CEN, 2004. ISO 13286-7 Unbound and Hydraulically Bound Mixtures. Part 7: Cyclic Load Triaxial Test for Unbound Mixtures. Belgium.

CEN, 2003. ISO 13286-4 Unbound and Hydraulically Bound Mixtures. Part 4: Test Methods for Laboratory Reference Density and Water Content. Vibrating hammer, Belgium.

Cerni, G., Cardone, F., Virgili, A., Camilli, S., 2012. Characterisation of permanent deformation behaviour of unbound granular materials under repeated triaxial loading. Construct. Build. Mater. 28, 79–87. https://doi.org/10.1016/j.conbuildmat.2011.07.066.

Chen, J., Yao, C., Wang, H., Ding, Y., Xu, T., 2018. Expansion and contraction of clogged open graded friction course exposed to freeze-thaw cycles and degradation of mechanical performance. Construct. Build. Mater. 182, 167–177. https://doi.org/10.1016/j.conbuildmat.2018.06.095.

Chowdhury, S.M.R.M., 2021. Evaluation of resilient modulus constitutive equations for unbound coarse materials. Construct. Build. Mater. 296, 123688 https://doi.org/10.1016/j.conbuildmat.2021.123688.

Chowdhury, S.M.R.M., Kassem, E., 2022. Estimation of resilient modulus constitutive model parameters for unbound coarse materials for MEPDG. J. Transport. Eng. Part B Pavements 148, 04022040. https://doi.org/10.1061/JPEODX.0000378.

Cong, L., Guo, G., Yang, F., Ren, M., 2020. The effect of hard segment content of polyurethane on the performances of polyurethane porous mixture. Int. J. Transp. Sci. Technol. 10, 254–265. https://doi.org/10.1016/j.ijtst.2020.07.003.

CRAMO, 2022. CRAMO [WWW Document]. URL. https://www.cramo.no/no.

Das, A., 2014. Analysis of pavement structures. In: Analysis of Pavement Structures, first ed. CRC Press, Boca Raton.

Dawson, A., 2008. Water in Road Structures. Springer, Notthingham.

Domitrović, J., Rukavina, T., Lenart, S., 2019. Effect of freeze-thaw cycles on the resilient moduli and permanent deformation of RAP/natural aggregate unbound base mixtures. Transp. Geotech. 18, 83–91. https://doi.org/10.1016/j.trgeo.2018.11.008.

Douglas, R.A., 2016. Low-Volume Road Engineering, first ed. CRC Press, Boca Raton.

Frey, H.C., Rasdorf, W., Lewis, P., 2010. Comprehensive field study of fuel use and emissions of nonroad diesel construction equipment. Transp. Res. Rec. J. Transp. Res. Board 2158, 69–76. https://doi.org/10.3141/2158-09.

Ghadimi, B., Nikraz, H., 2017. A comparison of implementation of linear and nonlinear constitutive models in numerical analysis of layered flexible pavement. Road Mater. Pavement Des. 18, 550–572. https://doi.org/10.1080/14680629.2016.1182055.

Ghorbani, B., Arulrajah, A., Narsilio, G., Horpibulsuk, S., 2020. Experimental investigation and modelling the deformation properties of demolition wastes subjected to freeze–thaw cycles using ANN and SVR. Construct. Build. Mater. 258, 119688 https://doi.org/10.1016/j.conbuildmat.2020.119688.

Gidel, G., Hornych, P., Chauvin, J.-J., Breysse, D., Denis, A., 2001. A new approach for investigating the permanent deformation behaviour of unbound granular material using the repeated load triaxial apparatus. Bull. Lab. Ponts Chaussees 4359, 5–21.

Gomes Correia, A., Winter, M.G., Puppala, A.J., 2016. A review of sustainable approaches in transport infrastructure geotechnics. Transp. Geotech. 7, 21–28. https://doi.org/10.1016/j.trgeo.2016.03.003.

Grenne, T., Grammeltvedt, G., Vokes, F.M., 1980. Ophiolites type sulphide deposits in the western Trondheim district, central Norwegian caledonides. In: International Ophiolite Symposium. Geological Survey Department, Cyprus, pp. 727–743.

Gulia, S., Goyal, P., Goyal, S.K., Kumar, R., 2019. Re-suspension of road dust: contribution, assessment and control through dust suppressants—a review. Int. J. Environ. Sci. Technol. 16, 1717–1728. https://doi.org/10.1007/s13762-018-2001-7.

Gullu, H., Hazirbaba, K., 2010. Unconfined compressive strength and post-freeze-thaw behavior of fine-grained soils treated with geofiber and synthetic fluid. Cold Reg. Sci. Technol. 62, 142–150. https://doi.org/10.1016/j.coldregions.2010.04.001.

Han, B., Ling, J., Shu, X., Song, W., Boudreau, R.L., Hu, W., Huang, B., 2019. Quantifying the effects of geogrid reinforcement in unbound granular base. Geotext. Geomembranes 47, 369–376. https://doi.org/10.1016/j.geotexmem.2019.01.009.

Hazirbaba, K., Gullu, H., 2010. California Bearing Ratio improvement and freeze-thaw performance of fine-grained soils treated with geofiber and synthetic fluid. Cold Reg. Sci. Technol. 63, 50–60. https://doi.org/10.1016/j.coldregions.2010.05.006.

Heidari, B., Marr, L.C., 2015. Real-time emissions from construction equipment compared with model predictions. J. Air Waste Manag. Assoc. 65, 115–125. https://doi.org/10.1080/10962247.2014.978485.

Hicks, R.G., Monismith, C.L., 1971. Factors influencing the resilient properties of granular materials. In: Highway Research Record, pp. 15–31.

Hoff, I., Bakløkk, L.J., Aurstad, J., 2003. Influence of laboratory compaction method on unbound granular materials. In: Dawson, A. (Ed.), 6th International Symposium on Pavements Unbound. Taylor & Francis, Nottingham.

Horpibulsuk, S., Suddeepong, A., Chinkulkijniwat, A., Liu, M.D., 2012. Strength and compressibility of lightweight cemented clays. Appl. Clay Sci. 69, 11–21. https://doi.org/10.1016/j.clay.2012.08.006.

Huang, J., Kogbara, R.B., Hariharan, N., Masad, E.A., Little, D.N., 2021. A state-of-the-art review of polymers used in soil stabilization. Construct. Build. Mater. 305, 124685 https://doi.org/10.1016/j.conbuildmat.2021.124685.

Huang, Y.H., 2004. Pavement Analysis and Design, second ed. Pearson, Upper Saddle River.

Hyde, A.F.L., 1974. Repeated Load Triaxial Testing of Soils. University of Nottingham.

Islam, K.M., Gassman, S., Rahman, M.M., 2020. Field and laboratory characterization of subgrade resilient modulus for pavement mechanistic-empirical pavement design

guide application. Transp. Res. Rec. J. Transp. Res. Board 2674, 921–930. https://doi.org/10.1177/0361198120926171.
Jones, D., 2017. Guidelines for the Selection, Specification, and Application of Chemical Dust Control and Stabilization Treatments on Unpaved Roads. Davis.
Jones, D., 1999. Holistic approach to research into dust and dust control on unsealed roads. Transp. Res. Rec. J. Transp. Res. Board 1652, 3–9. https://doi.org/10.3141/1652-35.
Kestler, M.A., 2009. Stabilization Selection Guide for Aggregate and Native-Surfaced Low Volume Roads. Washington, DC.
Khoeini, S., Dessouky, S., Papagiannakis, A.T., Walubita, L., Tahami, S.A., Gholikhani, M., 2019. Using polymer-based mixes as alternative to asphalt mixes in low volume roads. Construct. Build. Mater. 204, 177–183. https://doi.org/10.1016/j.conbuildmat.2019.01.124.
Kim, J.-K., Han, S.H., Song, Y.C., 2002a. Effect of temperature and aging on the mechanical properties of concrete Part I . Experimental results. Cement Concr. Res. 32, 1087–1094. https://doi.org/10.1016/S0008-8846(02)00744-5.
Kim, J.-K., Hun Han, S., Kyun Park, S., 2002b. Effect of temperature and aging on the mechanical properties of concrete: Part II. Prediction model. Cement Concr. Res. 32, 1095–1100. https://doi.org/10.1016/S0008-8846(02)00745-7.
Komatsu, 2009. Specifications and Application Handbook. Tokyo.
Kunz, B.K., Little, E.E., Barandino, V.L., 2021. Aquatic toxicity of chemical road dust suppressants to freshwater organisms. Arch. Environ. Contam. Toxicol. 82, 294–305. https://doi.org/10.1007/s00244-020-00806-y.
Latifi, N., Vahedifard, F., Ghazanfari, E., Horpibulsuk, S., Marto, A., Williams, J., 2018. Sustainable improvement of clays using low-carbon nontraditional additive. Int. J. GeoMech. 18, 04017162 https://doi.org/10.1061/(ASCE)GM.1943-5622.0001086.
Lekarp, F., Isacsson, U., Dawson, A., 2000a. State of the art. I: resilient response of unbound aggregates. J. Transport. Eng. 126, 66–75 https://doi.org/10.1061/(ASCE)0733-947X(2000)126:1(66).
Lekarp, F., Isacsson, U., Dawson, A., 2000b. State of the art. II: permanent strain response of unbound aggregates. J. Transport. Eng. 126, 76–83 https://doi.org/10.1061/(ASCE)0733-947X(2000)126:1(76).
Li, C., Ashlock, J.C., White, D.J., Vennapusa, P.K.R., 2019. Mechanistic-based comparisons of stabilised base and granular surface layers of low-volume roads. Int. J. Pavement Eng. 20, 112–124. https://doi.org/10.1080/10298436.2017.1321417.
Li, C., Vennapusa, P.K.R., Ashlock, J., White, D.J., 2017. Mechanistic-based comparisons for freeze-thaw performance of stabilized unpaved roads. Cold Reg. Sci. Technol. 141, 97–108. https://doi.org/10.1016/j.coldregions.2017.06.004.
Li, G., Hou, X., Zhou, Y., Ma, W., Mu, Y., Chen, D., Tang, L., 2021. Freeze-thaw resistance of eco-material stabilized loess. J. Mt. Sci. 18, 794–805. https://doi.org/10.1007/s11629-020-6308-8.
Little, L., Carlson, R.F., Connor, B., 2007. Tests of stabilization products for sandy soils from the national petroleum reserve – Alaska. Transp. Res. Rec. J. Transp. Res. Board 120–129.
Liu, J., Zhang, X., Li, L., Saboundjian, S., 2018. Resilient behavior of unbound granular materials subjected to a closed-system freeze-thaw cycle. J. Cold Reg. Eng. 32, 1–12 https://doi.org/10.1061/(ASCE)CR.1943-5495.0000142.
Lu, X., Isacsson, U., 2002. Effect of ageing on bitumen chemistry and rheology. Construct. Build. Mater. 16, 15–22 https://doi.org/10.1016/S0950-0618(01)00033-2.
Lunsford, G.B., Mahoney, J.P., 2001. Dust Control on Low Volume Roads. A Review of Techniques and Chemicals Used. Seattle.
Mallick, R.B., El-Korchi, T., 2013. Pavement Engineering. Principles and Practice, second ed. Taylor & Francis, Boca Raton.
Meijer, J.R., Huijbregts, M.A.J., Schotten, K.C.G.J., Schipper, A.M., 2018. Global patterns of current and future road infrastructure. Environ. Res. Lett. 13 https://doi.org/10.1088/1748-9326/aabd42.
Mohajerani, A., Suter, D., Jeffrey-Bailey, T., Song, T., Arulrajah, A., Horpibulsuk, S., Law, D., 2019. Recycling waste materials in geopolymer concrete. Clean Technol. Environ. Policy 21, 493–515. https://doi.org/10.1007/s10098-018-01660-2.
Muhammad, N., Siddiqua, S., 2022. Calcium bentonite vs sodium bentonite: the potential of calcium bentonite for soil foundation. Mater. Today Proc. 48, 822–827. https://doi.org/10.1016/j.matpr.2021.02.386.
Muresan, B., Capony, A., Goriaux, M., Pillot, D., Higelin, P., Proust, C., Jullien, A., 2015. Key factors controlling the real exhaust emissions from earthwork machines. Transport. Res. Part D 41, 271–287. https://doi.org/10.1016/j.trd.2015.10.002.
Myre, J., 2000. The use of cold bitumen stabilized base course mixes in Norway. In: Conference of the Baltic Road Association, pp. 1–14. Tallinn.
Newman, J.K., Tingle, J.S., Gill, C., McCaffrey, T., 2005. Stabilization of silty sand using polymer emulsions. Int. J. Pavements 4, 1–12.
NPRA, 2018. Håndbok N200 Vegbygging. Vegdirektoratet, Norway.
NPRA, 2014. Håndbok N200 Vegbygging. Vegdirektoratet, Norway.
Onyejekwe, S., Ghataora, G.S., 2015. Soil stabilization using proprietary liquid chemical stabilizers: sulphonated oil and a polymer. Bull. Eng. Geol. Environ. 74, 651–665. https://doi.org/10.1007/s10064-014-0667-8.
Parsakhoo, A., Hosseini, S.A., Lotfalian, M., Mohammadi, J., Salarijazi, M., 2020. Effects of molasses, polyacrylamide and bentonite on dust control in forest roads. J. For. Sci. 66, 218–225. https://doi.org/10.17221/41/2020-JFS.
Petkovic, G., Engelsen, C.J., Håøya, A.O., Breedveld, G., 2004. Environmental impact from the use of recycled materials in road construction: method for decision-making in Norway. Resour. Conserv. Recycl. 42, 249–264. https://doi.org/10.1016/j.resconrec.2004.04.004.
Pierre, P., Bilodeau, J.P., Légère, G., Doré, G., 2008. Laboratory study on the relative performance of treated granular materials used for unpaved roads. Can. J. Civ. Eng. 35, 624–634. https://doi.org/10.1139/L08-012.
Plati, C., 2019. Sustainability factors in pavement materials, design, and preservation strategies: a literature review. Construct. Build. Mater. 211, 539–555. https://doi.org/10.1016/j.conbuildmat.2019.03.242.
Poltue, T., Suddeepong, A., Horpibulsuk, S., Samingthong, W., Arulrajah, A., Rashid, A.S.A., 2020. Strength development of recycled concrete aggregate stabilized with fly ash-rice husk ash based geopolymer as pavement base material. Road Mater. Pavement Des. 21, 2344–2355. https://doi.org/10.1080/14680629.2019.1593884.
PON-CAT, 2022. PON-CAT [WWW Document]. URL. https://www.pon-cat.com/no.
Pranav, S., Lahoti, M., Shan, X., Yang, E., Muthukumar, G., 2022. Economic input-output LCA of precast corundum-blended ECC overlay pavement. Resour. Conserv. Recycl. 184, 106385 https://doi.org/10.1016/j.resconrec.2022.106385.
Prasara-A, J., Bridhikitti, A., 2022. Carbon footprint and cost analysis of a bicycle lane in a municipality. Glob. J. Environ. Sci. Manag. 8, 197–208 https://doi.org/10.22034/GJESM.2022.02.04.
Praticò, F., Saride, S., Puppala, A., 2011. Comprehensive life-cycle cost analysis for selection of stabilization alternatives for better performance of low-volume roads. Transp. Res. Rec. J. Transp. Res. Board 2204, 120–129 https://doi.org/10.3141/2F2204-16.
Qu, Y., Chen, G., Niu, F. un, Ni, W., Mu, Y., Luo, J., 2019. Effect of freeze-thaw cycles on uniaxial mechanical properties of cohesive coarse-grained soils. J. Mt. Sci. 16, 2159–2170. https://doi.org/10.1007/s11629-019-5426-7.
RAMIRENT, 2022. RAMIRENT [WWW Document]. URL. https://www.ramirent.no/.
Rosa, M.G., Cetin, B., Edil, T.B., Benson, C.H., 2017. Freeze–thaw performance of fly ash–stabilized materials and recycled pavement materials. J. Mater. Civ. Eng. 29, 1–13 https://doi.org/10.1061/(ASCE)MT.1943-5533.0001844.
Santoni, R.L., Tingle, J.S., Nieves, M., 2005. Accelerated strength improvement of silty sand with nontraditional additives. Transp. Res. Rec. J. Transp. Res. Board 34–42, 1936, https://doi.org/10.1177/2F0361198105193600105.
Santoni, R.L., Tingle, J.S., Webster, S.L., 2002. Stabilization of silty sand with nontraditional additives. Transp. Res. Rec. J. Transp. Res. Board 1787, 61–70 https://doi.org/10.3141/2F1787-07.
Silyanov, V., Sodikov, J.I., 2017. Highway functional classification in ICS countries. In: Dell'Acqua, G., Wegman, F. (Eds.), Transport Infrastructure and Systems - Proceedings of the AIIT International Congress on Transport Infrastructure and Systems, TIS 2017. Taylor & Francis, Rome, pp. 411–417. https://doi.org/10.1201/9781315281896.
Silyanov, V., Sodikov, J.I., Kiran, R., Sadikov, I., 2020. An overview road data collection, visualization, and analysis from the perspective of developing countries. IOP Conf. Ser. Mater. Sci. Eng. 832 https://doi.org/10.1088/1757-899X/832/1/012056.
Simonsen, E., Isacsson, U., 1999. Thaw weakening of pavement structures in cold regions. Cold Reg. Sci. Technol. 29, 135–151. https://doi.org/10.1016/S0165-232X(99)00020-8.
Simonsen, E., Janoo, V.C., Isacsson, U., 2002. Resilient properties of unbound road materials during seasonal frost conditions. J. Cold Reg. Eng. 16, 28–50 https://doi.org/10.1061/(ASCE)0887-381X(2002)16:1(28).
Tan, E.H., Zahran, E.M.M., Tan, S.J., 2020. A review of chemical stabilisation in road construction. IOP Conf. Ser. Mater. Sci. Eng. 943 https://doi.org/10.1088/1757-899X/943/1/012005.
Tao, M., Mohammad, L.N., Nazzal, M.D., Zhang, Z., Wu, Z., 2010. Application of shakedown theory in characterizing traditional and recycled pavement base materials. J. Transport. Eng. 136, 214–222 https://doi.org/10.1061/(ASCE)0733-947X(2010)136:3(214).
Thom, N., 2014. Principles of Pavement Engineering, second ed. ICE, London.
Tian, S., Tang, L., Ling, X., Kong, X., Li, S., Cai, D., 2019. Cyclic behaviour of coarse-grained materials exposed to freeze-thaw cycles: experimental evidence and evolution model. Cold Reg. Sci. Technol. 167, 102815 https://doi.org/10.1016/j.coldregions.2019.102815.
Tingle, J.S., Newman, J.K., Larson, S.L., Weiss, C.A., Rushing, J.F., 2007. Stabilization mechanisms of nontraditional additives. Transp. Res. Rec. J. Transp. Res. Board 59–67, 1989, https://doi.org/10.3141/2F1989-49.
Tingle, J.S., Santoni, R.L., 2003. Stabilization of clay soils with nontraditional additives. Transp. Res. Rec. J. Transp. Res. Board 1819, 72–84 https://doi.org/10.3141/2F1819b-10.
Titi, H.H., Matar, M.G., 2018. Estimating resilient modulus of base aggregates for mechanistic-empirical pavement design and performance evaluation. Transp. Geotech. 17, 141–153. https://doi.org/10.1016/j.trgeo.2018.09.014.
Trani, M.L., Bossi, B., Gangolells, M., Casals, M., 2016. Predicting fuel energy consumption during earthworks. J. Clean. Prod. 112, 3798–3809. https://doi.org/10.1016/j.jclepro.2015.08.027.
Utleiesenteret, 2022. Utleiesenteret [WWW Document]. URL. https://www.utleiesenteret.no/.
Uys, R., Truter, L., Van Zyl, G., 2011. Various additives used as alternative to conventional road construction. Transp. Res. Rec. J. Transp. Res. Board 2204, 179–185. https://doi.org/10.3141/2204-23.
van der Merwe Steyn, W., Visser, A., 2011. Evaluation of sustainability of low-volume roads treated with nontraditional stabilizers. Transp. Res. Rec. J. Transp. Res. Board 2204, 186–193. https://doi.org/10.3141/2204-24.
Werkmeister, S., Dawson, A., Wellner, F., 2005. Permanent deformation behavior of granular materials and the shakedown concept. Transp. Res. Rec. J. Transp. Res. Board 1757, 75–81 https://doi.org/10.3141/2F1757-09.
White, D.J., Vennapusa, P., 2013. Low-cost Rural Surface Alternatives Literature Review and Recommendations. Ames.
Wirtgen Group, 2022. Wirtgen Group [WWW Document]. URL. https://www.wirtgen-group.com/en-no/.
Xiao, R., Jiang, X., Wang, Y., He, Q., Huang, B., 2021. Experimental and thermodynamic study of alkali-activated waste glass and calcium sulfoaluminate cement blends:

Shrinkage, efflorescence potential, and phase assemblages. J. Mater. Civ. Eng. 33, 1–14 https://doi.org/10.1061/(ASCE)MT.1943-5533.0003941.

Xiao, R., Jiang, X., Zhang, M., Polaczyk, P., Huang, B., 2020a. Analytical investigation of phase assemblages of alkali-activated materials in CaO-SiO2-Al2O3 systems: the management of reaction products and designing of precursors. Mater. Des. 194, 108975 https://doi.org/10.1016/j.matdes.2020.108975.

Xiao, R., Polaczyk, P., Zhang, M., Jiang, X., Zhang, Y., Huang, B., Hu, W., 2020b. Evaluation of glass powder-based geopolymer stabilized road bases containing recycled waste glass aggregate. Transport. Res. Rec. 2674, 22–32. https://doi.org/10.1177/0361198119898695.

Xiao, R., Shen, Z., Si, R., Polaczyk, P., Li, Y., Zhou, H., Huang, B., 2022. Alkali-activated slag (AAS) and OPC-based composites containing crumb rubber aggregate: physico-mechanical properties , durability and oxidation of rubber upon NaOH treatment. J. Clean. Prod. 367, 132896 https://doi.org/10.1016/j.jclepro.2022.132896.

Xuan, D.X., Houben, L.J.M., Molenaar, A.A.A., Shui, Z.H., 2012. Mechanical properties of cement-treated aggregate material – a review. Mater. Des. 33, 496–502 https://doi.org/10.1016/j.matdes.2011.04.055.

Zhang, T., Cai, G., Liu, S., 2017. Application of lignin-based by-product stabilized silty soil in highway subgrade: a field investigation. J. Clean. Prod. 142, 4243–4257. https://doi.org/10.1016/j.jclepro.2016.12.002.

Zhang, T., Yang, Y.L., Liu, S.Y., 2020. Application of biomass by-product lignin stabilized soils as sustainable geomaterials: a review. Sci. Total Environ. 728, 138830 https://doi.org/10.1016/j.scitotenv.2020.138830.

Zhang, Y., Gong, H., Jiang, X., Lv, X., Xiao, R., Huang, B., 2021. Environmental impact assessment of pavement road bases with reuse and recycling strategies: a comparative study on geopolymer stabilized macadam and conventional alternatives. Transport. Res. Transport Environ. 93, 102749 https://doi.org/10.1016/j.trd.2021.102749.

Zhang, Y., Johnson, A.E., White, D.J., 2016. Laboratory freeze-thaw assessment of cement, fly ash, and fiber stabilized pavement foundation materials. Cold Reg. Sci. Technol. 122, 50–57. https://doi.org/10.1016/j.coldregions.2015.11.005.